UNIVERSIDADE DE LISBOA
FACULDADE DE CIÊNCIAS
DEPARTAMENTO DE BIOLOGIA ANIMAL

The role of *Down syndrome cell adhesion molecule 1* for the bacterial microbiota of *Tribolium castaneum*

Luís Manuel Macedo da Silva

Mestrado em Biologia Evolutiva e do Desenvolvimento

Dissertação orientada por:
Professor Dr. Joachim Kurtz | University of Münster, Germany
Professor Dr. Élio Sucena | University of Lisbon, Portugal

Acknowledgement

I would first like to thank Professor Dr. Joachim Kurtz for the opportunity to do the thesis in his group and for all the support he provided along the way.

I would especially like to thank Dr. Sophie Armitage for her tireless guidance and open door whenever I had questions or problems.

I am also grateful to the Tribolium group, namely Barbara, Kevin, Diana, Nora and Rasha for the help in the laboratory, as well as all the fruitful discussions and troubleshooting throughout the project.

I would also like to thank Professor Élio Sucena and Sólveig Thorsteinsdóttir for all the challenges and help they provided throughout the Master.

Finally, I must also thank my friends and family for all the support, long conversations and mostly for the patience they had.

Thank you very much everyone! I will be always grateful.

Abstract

Hosts establish different types of interactions with the elements of their microbiota. These interactions can be broadly classified as positive, neutral or negative and shaped the evolution of the immune system. Negative interactions may lead to host-parasite coevolution. While the host may only survive and reproduce by exhibiting more efficient immune responses, the parasite requires novel ways of dodging the host's immune system. On the other hand, positive interactions can evolve to the point where the lack of specific microorganisms may interfere with tissue development, immunity or resistance to pathogens. Neutral interactions are not only difficult to define but are also thought to be dynamic and could evolve to either positive or negative interactions. Consequently, the host needs to be able to differentiate between harmful and beneficial microbes. This identification is thought to be performed through pattern recognition receptors that recognise microbe-associated molecular patterns and other environmental cues, enabling an appropriate response from the host.

Dscam1 is a gene expressed in neurons and essential to the correct development of neuronal circuits. Through alternative splicing, it is able to originate around 18.000 isoforms in *Drosophila melanogaster* and 15.000 in *Tribolium castaneum*. More recently, its expression was observed in immune cells and tissues of some invertebrates. Recent studies have shown differential isoforms expression after infection by different classes of bacteria. Hence, it was suggested that Dscam1 may work as a pattern recognition receptor, opsonin and/or bacteria regulator. Concerning bacteria regulation, there are studies in *Anopheles gambiae* that show a proliferation of gut bacteria after a *Dscam1* knock-down. In the same model, overexpression of bacteria-induced Dscam1 isoforms resulted in a reduction of bacteria in the haemolymph. The above-mentioned results suggest that Dscam1 is involved in negative regulation of bacteria. Nonetheless, there is also evidence suggesting a decrease in the intracellular parasites and no effect on extracellular bacteria after *Dscam1* knock-down in *Laodelphax striatellus*.

Hence, I aimed to clarify the role of Dscam1 in the dynamics of *Tribolium castaneum* bacterial microbiota. This was achieved through *Dscam1* knock-down and bacterial load analysis through RTqPCR for the bacterial *16S rRNA* at three time-points of the beetle development: 15-days old larvae, 23-days old pupae and 30-days old adults.

Our results show that a *Dscam1* knock-down does not affect the total amount of bacteria in the beetle in any of the three developmental time-points analysed. This is in agreement with previous studies. Nevertheless, a correlation between the relative expression of the bacterial *16S rRNA* and *Dscam1* was observed. The correlation had a negative tendency: a higher expression of *Dscam1* was correlated with a lower expression of *16S rRNA* and therefore less bacteria in the system. Such a tendency was also observed in Dong and colleagues' studies on adult mosquitoes. A knock-down may not be sufficient to disturb a robust system capable of bacterial regulation in this model. Further analyses of the composition of bacterial microbiota are required to clarify the role of Dscam1 in bacterial regulation in *T. castaneum*. It is for example possible that changes occur in the proportion of different bacterial taxa.

Keywords: Dscam, Tribolium castaneum, 16S rRNA, microbiota, insect immunity

Resumo

Organismos multicelulares estabelecem diversos tipos de interações com microrganismos. Estas interações podem ser positivas, neutras ou negativas para o hospedeiro. As diferentes interações moldaram a evolução do sistema imunitário. Interações negativas levam a uma co-evolução parasita-hospedeiro. Os hospedeiros necessitam de apresentar mecanismos e respostas imunes mais eficientes para sobreviverem e reproduzirem-se, enquanto que os parasitas requerem novas formas de escapar ou resistir ao sistema imune do hospedeiro e infeta-lo. Contudo, grande parte dos organismos estabelecem interações neutras ou benéficas para o hospedeiro. Num cenário de mutualismo, a interação pode ser necessária ao desenvolvimento de estruturas ou crucial para que o hospedeiro apresente uma imunidade eficiente. No caso das interações neutras, pensa-se que sejam dinâmicas e facilmente possam evoluir para uma interação positiva/negativa. Desta forma, os diversos tipos de interação levaram à evolução do sistema imunitário e à necessidade de uma forma de diferenciação entre microrganismos benéficos e prejudiciais por parte do hospedeiro.

Uma possível explicação para a diferenciação entre diferentes tipos de interação foi sugerida recentemente por Lazzaro and Rolff. Esta hipótese sugere que o sistema imunitário do hospedeiro é capaz de ajustar o tipo de resposta conforme o rácio de sinais a que é sujeito. Enquanto que uma ferida levaria à expressão de sinais de danos, um simbionte apenas apresentaria os seus padrões moleculares associados a micróbios a receptores nas células do hospedeiro. Contudo, um parasita apresentaria não só os padrões moleculares associados a micróbios, como também causaria danos no tecido infetado, levando à expressão de sinais de danos pelas células. Assim, o estabelecimento de interações positivas e respostas imunes apropriadas dependem do reconhecimento por parte do hospedeiro e possivelmente de um balanço entre diferentes sinais. A diferenciação entre diferentes microrganismos deverá depender de receptores que permitam o reconhecimento e levem à produção uma resposta adequada. Dscam1 tem sido sugerido como possível receptor de reconhecimento dada a grande quantidade de isoformas que é capaz de produzir por *alternative splicing*.

Down syndrome cell adhesion molecule 1 (*Dscam1*) é um gene expresso em neurónios e em alguns invertebrados em células e tecidos do sistema imunitário. Por *alternative splicing* é capaz de originar cerca de 18.000 isoformas em *Drosophila melanogaster* e 15.000 em *Tribolium castaneum*. Esta proteína é essencial para o desenvolvimento de circuitos neuronais A grande variabilidade de isoformas permite a identificação e consequente repulsão de dendrites-irmãs. Isto assegura que as dendrites cubram a maior área possível e assim estabeleçam um correto circuito neuronal. A análise da estrutura proteica de Dscam1 permitiu identificar dois epítopos (I e II). O epítopo I está envolvido em interações homofílicas no sistema nervoso e é bastante conservado, coerente com a sua função no desenvolvimento de circuitos neuronais e elevada pressão seletiva para um grupo limitado de isoformas. Por outro lado, o epítopo II apresenta grande variabilidade na sua sequência. Dada esta variabilidade, foi proposto que este epítopo poderá estar envolvido no reconhecimento de microrganismos. Recentemente, vários estudos têm proposto não só uma função no reconhecimento de microrganismos, mas também como possível opsonina e/ou regulador de bactérias no hospedeiro. Sabe-se que diferentes bactérias induzem a expressão de diferentes isoformas de Dscam1. Contudo, ainda permanece um mistério como é que é produzida esta expressão diferencial e qual a sua função na imunidade de invertebrados. No mosquito *Anopheles gambiae*, um knock-down de *Dscam1* levou a uma redução no index de fagocitose, bem como uma proliferação das bactérias na hemolinfa. Seis anos mais tarde, ao sobre-expressarem uma isoforma de *Dscam1* induzida na presença de bactérias, observaram uma redução nas bactérias no mosquito. Porém, há resultados contraditórios. Em *Laodelphax striatellus* após o knock-down de *Dscam1*, observa-se uma redução na infeção por parasitas intracelulares como *Wolbachia* e nenhuma alteração no número de bactérias extracelulares.

Deste modo, o objetivo desta tese foi clarificar o papel de Dscam1 na microbiota bacteriana de *T. castaneum*. Para tal, procedeu-se ao *knock-down* de *Dscam1* e posteriores análises à quantidade total de microbiota bacteriana em três pontos de desenvolvimento: estádio de larva (15 dias pós-oviposição); estádio de pupa (23 dias pós-oviposição) e estádio de adulto (30 dias pós-oviposição). Através de RTqPCR foi possível quantificar quer o *knock-down* de *Dscam1*, quer a quantidade de bactérias em cada tratamento utilizando como proxy o gene bacteriano *16S* rRNA.

Os resultados deste projeto mostram que em *Tribolium castaneum*, um *knock-down* de *Dscam1* parece não afetar a quantidade total de bactérias. Isto foi observado para os três pontos de desenvolvimento analisados. Estes resultados sugerem que neste modelo, Dscam1 poderá não regular a flora bacteriana como observado em mosquito. No entanto, foi observada uma forte correlação entre a expressão relativa do *16S rRNA* bacteriano e a expressão relativa do *Dscam1* para dois dos três pontos de desenvolvimento. A correlação é de caráter negativo: uma maior expressão de *Dscam1* está correlacionada com uma menor expressão de *16S rRNA* e por consequente, menor quantidade de bactérias no sistema. Esta tendência foi observada por Dong e colegas em mosquitos adultos. Assim, é possível que *Dscam1* faça parte de um sistema robusto que reconhece/regula bactérias e não é afetado por baixos níveis de Dscam1. É ainda possível que caso Dscam1 tenha uma função no reconhecimento/regulação de bactérias, haja outros receptores com função redundante que possam compensar a falta deste em particular.

De forma a responder a estas questões, um estudo mais exaustivo onde se analisasse também a composição bacteriana após *knock-down* de *Dscam1* seria necessário. É possível que não se observe alterações na quantidade total de bactérias, mas sim diferentes proporções de cada classe após redução de *Dscam1*. Seria expectável que classes reguladas por *Dscam1* teriam as suas proporções aumentadas face a outras classes. Dada a evidência de forte competição bacteriana dentro da microbiota, é possível que não se observe diferenças significativas no número total de bactérias, mas sim diferenças na sua identidade.

Palavras-chave: Dscam, Tribolium castaneum, 16S rRNA, microbiota, imunidade

Table of Contents

List of figures

List of tables

List of abbreviations

AMP	Antimicrobial peptide
asnA	*Asparginase synthetas*e
DSCAM	Down syndrome cell adhesion molecule
DSCAM1	Down syndrome cell adhesion molecule form 1
dsRNA	Double strand RNA
IMD	Immune deficiency pathway
LPS	Lipopolysaccharide
MAMP	Microbe associated molecular pattern
min	Minutes
PCR	Polymerase chain reaction
PRR	Pathogen recognition receptor
qPCR	Quantitative polymerase chain reaction
RFLP	Restriction fragment length polymorphism
RNAi	RNA interference
ROS	Reactive oxygen species
Rp49	*Ribosomal protein 49*
Rpl13a	*Ribosomal protein L13a*
RT	Reverse transcription
RTqPCR	Real-time quantitative polymerase chain reaction
s	Seconds
TGIP	Trans-generational immune priming
WSSV	White spot syndrome virus

1. Introduction

1.1 - Evolution of immunity

Since early in eukaryotic evolution, multicellular organisms have been exposed to a high diversity of microorganisms. The term microbiota encompasses all the mutualistic, commensal and pathogenic microorganisms that live inside or on a host (Lederberg & McCray 2001). These microbes can include protozoa, bacteria, viruses or fungi. Classically, host-microbe interactions are seen as mostly agonistic and a decisive evolutionary driving-force (Woolhouse et al. 2002; Obbard et al. 2009). Pathogens evolved to lucratively parasitize the host, negatively affecting their fitness (Hornef et al. 2002). The host-parasite antagonism may lead to an evolutionary arms race, known as Red Queen hypothesis (Van Valen 1973). Hosts may only survive and reproduce by exhibiting more efficient immune mechanisms, while parasites require novel ways of dodging the hosts' immunity to successfully infect them. It is fair to assume host-parasite coevolution presents a strong selective pressure in the natural environment and has led to the selection of a broad range of responses and in part to the evolution of the immune system (Dybdahl & Lively 1998; Kaufman 2010; Obbard et al. 2009). Nonetheless, most microbes are actually neutral or beneficial to the host (Lee & Mazmanian 2010). Almost every environmentally exposed host surface is bursting with commensal and beneficial microbes but most reside in their gut (Turnbaugh et al. 2007; Sommer & Bäckhed 2013). In *Drosophila*, there is evidence for the contribution of commensal bacteria for mate preference (Sharon et al. 2010). In mice, commensal microbiota found in the ocular surface seem to elicit an interleukin-17 response, central to the tissue immune homeostasis (Leger et al. 2017). Nonetheless, in some cases it may be difficult to draw the line between a neutral and positive/negative interaction and its dynamics may allow a neutral interaction to evolve to either a mutualistic or pathogenic scenario (Hooper & Gordon 2001). Regarding mutualistic interactions, they may evolve to the point where the lack/absence of the microbe can lead to the incorrect development of tissues, immunological disequilibrium or even higher host susceptibility to pathogens (Sommer & Bäckhed 2013; Mazmanian et al. 2005; Teixeira et al. 2008; Weiss et al. 2013; Dong et al. 2009). As an example, the bacteria *Vibrio fischeri* releases tracheal cytotoxins that act in synergy with lipopolysaccharides (LPS) as a morphogen, inducing the morphogenesis of the light organ in the squid *Euprymna scolopes* (Koropatnick et al. 2004). In mice, the gut bacteria *Bacteroides fragilis* releases a polysaccharide essential to the correct maturation of T cells, as well as the lymphoid organogenesis (Mazmanian et al. 2005). *Wolbachia* is a genus of wide-spread endosymbionts among arthropods that can have both parasitic and mutualistic interactions. Its presence has been linked to enhanced resistance towards a variety of RNA viruses in *Drosophila* (Teixeira et al. 2008). Hence it is fair to assume, that symbionts are equally important to the shaping of the immune system (Bosch 2014).

Taking the insects as an example, the gut colonization can be achieved by very distinct paths: host diet, vertical transmission (parental-offspring), cropophagy and in social insects also by horizontal (social) transmission (Engel & Moran 2013). Moreover, the insect guts can be particularly unstable over the lifetime of an organism as a result of the remodelling upon metamorphosis and moulting. In *Tribolium castaneum* there is evidence for changes in the bacterial phyla proportions across development (Futo 2016). During the remodelling events, the gut microbiota is nearly or completely eliminated (Engel & Moran 2013) and gained later in life (Hammer et al. 2014).

Although, the bacterial microbiome is environmentally acquired, it does not simply reflect the microbial intake of the host (Chandler et al. 2011). Hence, the host exerts significant control over its composition. A study in Hydra has shown that species-specific microbial communities are shaped

through the expression of species-specific antimicrobial peptides (AMPs) patterns (Fraune & Bosch 2007; Franzenburg et al. 2013). In *Drosophila*, the immune pathways responsible for this regulation can also be modulated, namely through the repression of AMPs transcription by *caudal* (Ryu et al. 2008). Host microbial regulation may lead to population and species-specific bacterial phylogenetic clusters. The latter was defined as core microbiota (Turnbaugh et al. 2007) and was found in some populations and species (Dishaw et al. 2014; Brucker & Bordenstein 2012; Ochman et al. 2010; Thongaram et al. 2005). However, the concept is still controversial since there are also conflicting results (Chandler et al. 2011; Corby-Harris et al. 2007; Wong et al. 2013) and the study of natural microbial communities in the laboratory is problematic. Furthermore, the microbiota can be relatively flexible and shaped by external factors, such as host diet, host pathobiology or the environment itself (Turnbaugh et al. 2007; Yun et al. 2014).

Thus, it seems that the host immune system evolved to not only destroy prejudicial microbes, but also to maintain and regulate strong and stable relationships with beneficial ones (Bosch 2014). Both driving-forces are critical to the maintenance of the host's homeostasis but how it evolved to identify each one of the two types of microbes still remains unclear. A possible explanation for the differentiation between harmful and beneficial microbes was recently suggested by Lazzaro and Rolff (2011). According to this hypothesis, a pathogen would release microbe-associated molecular patterns (MAMPs) but also induce the infected tissue to release "danger signals" (Fig. 1.1). On the other hand, a symbiont would release MAMPs but not cause any damage and therefore no "danger signals" would be released from the tissue cells. A natural wound would only induce the production of "danger signals". This way, the balance between different elicitors could indicate what type of response should take place (Lazzaro & Rolff 2011).

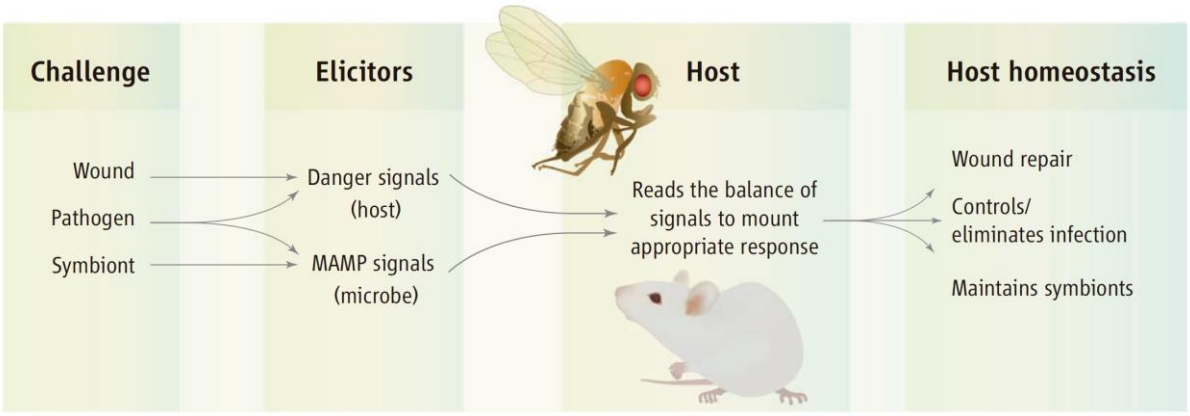

Figure 1.1 - Host differentiation between pathogens and symbionts through elicitor ratios. A wound only induces the production of "danger signals" by the host tissue, while symbionts only display MAMPs without causing damage to the host. Pathogens invasion exhibits both MAMPs and induces "danger signals" production, leading to the activation of an immune response by the host. The balance between the different elicitors may indicate what kind of response should take place. Figure adapted from Lazzaro & Rolff (2011).

1.2 - Insect immunity

Insects have evolved different lines of defences that interact in synergy to protect the organism: i) behavioural mechanisms, such as pathogens avoidance; ii) physical barriers, for instance the chitin exoskeleton; and lastly, iii) a wide range of immunological responses (Siva-Jothy et al. 2005).

Once a parasite has breached the insect outer barriers, such as the cuticle, the immune system can be activated. Host immune system activation is dependent on pathogen recognition. Recognition is

based on MAMPs not found in the host, allowing a distinction between host cells and different classes of microorganisms (Lazzaro & Rolff 2011; Medzhitov & Janeway 1997). MAMPs may include lipopolysaccharides and peptidoglycans. After pattern recognition through host pattern recognition receptors (PRRs), an appropriate response can be initiated (Schmid-Hempel 2005).

Invertebrates lack the adaptive branch of the immune system, as well as all their elements. Consequently they rely on a wide range of innate immune responses (Schmid-Hempel 2005). These immune responses can be categorized into cellular or humoral. Cellular immunity is based on haemocytes, the phagocytic cells of invertebrates. After pathogen recognition, phagocytosis takes place. Depending on the pathogen features, such as size, different strategies may be applied. In the presence of small pathogens, multiple haemocytes can attack the intruder, forming nodules, called nodulation. In the presence of larger pathogens, the haemocytes will form a capsule around it, called encapsulation. Both nodules and capsules go through a process of melanisation, where the pathogen is enclosed with melanin and destroyed with reactive oxygen species (ROS) (Lavine & Strand 2002; Marmaras & Lampropoulou 2009). ROS are one of the main insect humoral responses. They are a by-product during the activation of the melanisation cascade in the haemocytes (Cerenius & Söderhäll 2004). Another crucial mechanism of humoral immunity is the production of AMPs. These are found throughout the tree of life (Zasloff 2002), as a fundamental innate defence mechanism. These small molecules interfere with the metabolism of various bacterial pathogens in processes such as nucleic acid synthesis or enzyme activity (Mylonakis et al. 2016). In insects, AMPs are produced in the fat body at each infection and secreted into the haemolymph. Their activity remains for several days after the infection, protecting the organism from a re-infection by the pathogen (Makarova et al. 2016). In *Drosophila*, different classes of bacteria are thought to activate different pathways through PRRs binding (Lemaitre & Hoffmann 2007). Toll, Immune deficiency (IMD) and JAK/STAT pathways are known to differentially regulate AMP synthesis (Hillyer 2016). This results in the expression of an AMP pattern more effective against the class of pathogens currently infecting the host. However, not all insects express AMPs so distinctly. *T. castaneum* seems to have a more promiscuous AMP activation, through the usage of both Toll and IMD pathways (Yokoi et al. 2012).

Since invertebrates lack the adaptive machinery, it was thought that invertebrates could only rely on the generalized immune responses mentioned above (Schmid-Hempel 2005). However, a study (Kurtz & Franz 2003) has shown that in fact invertebrates also possess a form of immune memory, later called immune priming (Little & Kraaijeveld 2004). In this study, copepods *Macrocyclops albidus* were infected with the tapeworm *Schistocephalus solidus*. Two treatment groups took place. Both groups were first primed with the parasite and 2 days later one of the group was infected by a sibling *S. solidus* (genetically similar to the priming parasite), while the other group was infected by an unrelated *S. solidus* (genetically non-similar). There was a reduction in the reinfection success and intensity for the first group, compared to the latter. Hence, the immune system of the copepods was able to respond more efficiently after being presented for a second time with a sibling parasite (Kurtz & Franz 2003), which indicates that a form of specific memory exists. Immune priming has been defined as an enhanced protection resulting from past experience with a pathogen (Kurtz 2005). Evidence has been found suggesting this phenomenon may happen not only in invertebrates but also in vertebrates and plants (Paust & Von Andrian 2011; Spoel & Dong 2012). Invertebrate immune priming has now been demonstrated in a wide range of species (Contreras-Garduño et al. 2016; Milutinović et al. 2016). This phenomenon can occur not only within a generation but also across generations leading to stronger immune reactions or improved resistance of the offspring, which is then called trans-generational immune priming (TGIP) (Zanchi et al. 2011; Eggert et al. 2014; Roth et al. 2010; Trauer-Kizilelma & Hilker 2015). In *T. castaneum* it was shown that oral priming previous to infection with *Bacillus thurigiensis* leads to a shift in the gene expression (Greenwood et al. 2017), presumably caused by a more targeted response instead of a more generalized reaction from a non-

primed individual. The gene expression is also dependent on the infection route taken by the pathogen and the host population (Behrens et al. 2014).

It has been proposed that microbiota may also have a role in oral immune priming. Rodrigues *et al*. (2010) observed that primed *Anopheles gambiae* mosquitoes subjected to antibiotics treatment had an increase in *Plasmodium* parasites, as well as lower phagocytic activity, compared to the treatment without antibiotics (Rodrigues et al. 2010). In addition, Futo and colleagues (2015) observed that *T. castaneum* larvae with lowered microbial loads (after sterilization) showed decreased survival upon a secondary challenge with *Bacillus thurigiensis* compared to non-sterilized larvae. Furthermore, if the larvae were allowed to re-colonise themselves with gut microbiota after sterilisation and before priming-challenge, the survival after challenge was the same as the group where the microbiota were not manipulated (Futo et al. 2015). Both results suggest that host-associated microbiota is crucial to immune priming and may boost the immune response. Also, a study in bumblebees (Koch & Schmid-Hempel 2012) showed that different gut microbiota composition may lead to specific resistance against different pathogen strains, reinforcing the importance of microbiota in relation to immunity.

1.3 Dscam1: Down syndrome cell adhesion molecule 1

DSCAM was originally found in humans as a new class of neural cell adhesion molecules expressed within the nervous system (Yamakawa et al. 1998). Given its location on chromosome 21 and specific expression, it is thought to contribute to the neuroanatomic abnormalities found in Down syndrome (Yamakawa et al. 1998; Delabar et al. 1992).

A *Drosophila melanogaster* homolog of human DSCAM was later isolated and named Dscam (Schmucker et al. 2000). Both transmembrane proteins are members of the Immunoglobulin superfamily, one of the largest class of surface receptor proteins found in animals (Schmucker & Chen 2009). There are four Dscam paralogs in Drosophila (form 1-4). However, only Dscam1 possess a high diversity of isoforms originated through alternative splicing of the high variably cluster of exons (exons 4, 6, 9 and 17) (Schmucker et al. 2000; Hattori et al. 2008). Dscam1 structure consists of ten immunoglobulin-like domains, six type III fibronectin domains, a single transmembrane segment and a cytoplasmic domain. In *D. melanogaster* it is predicted to encode 18,612 distinct axon guidance receptors through alternative splicing of 95 exons (Schmucker et al. 2000). Although, the domain structure of the vertebrate DSCAM and Dscam1 is quite similar, the latter presents a bigger sequence diversity in their extracellular region (Schmucker et al. 2000). The alternative exons that encode for hypervariability seem to be present in insects and crustaceans but not in vertebrates (Brites et al. 2013). Up to now, this hypervariable form has been found in numerous pancrustaceans, including *T. castaneum* (Ng et al. 2014; Watson et al. 2005). However, the number of alternatively spliced exons varies throughout the pancrustaceans (Armitage & Brites 2016). A phylogenetic analysis of Dscam hypothesised that this hypervariable form may have appeared in the common ancestor of Pancrustacea (Armitage et al. 2012; Armitage & Brites 2016) (Figure 1.2C).

Dscam1 is expressed throughout sensory and central nervous system neurons (Fuerst et al. 2009; Schmucker & Chen 2009). Its first discovered role was to mediate the sister-dendrites repulsion in neuronal wiring (Schmucker et al. 2000; Lawrence Zipursky & Grueber 2013). During neuronal wiring, specific cells express Netrin-B as a guidance cue perceived by the netrin-receptor Frazzled in the neurons' membrane (Hiramoto et al. 2000). At the same time, unique patterns of Dscam1 isoforms are also expressed in the cell membranes of neurons. This patterning allows the neuron to discriminate between its own neurites and neurites from another neuron (Lawrence Zipursky & Grueber 2013). Dscam1 in synergy with the Netrin/Frazzled system assures the spreading of the dendrites throughout

the neuronal field, maximizing territory coverage (Lawrence Zipursky & Grueber 2013; Hiramoto et al. 2000; Matthews & Grueber 2011). In absence of Dscam1, the dendrites tend to "hypertarget" the source of Netrin and not establish a correct neural circuit (Matthews & Grueber 2011). Homophilic binding of the extracellular region has been shown to result in the repulsion of neurons, whereas heterophilic binding in the nervous system leads to tiling of two neurons (Hughes et al. 2007). In *Drosophila*, when the ectodomain diversity was eliminated, defects during neural wiring arose (Hattori et al. 2007). Meijers and colleagues analysed the protein structure of Dscam at *Drosophila* interspecies level and noticed that the epitope I, involved in homophilic interactions in the nervous system, presents a highly conserved amino acid sequence. This observation is consistent with a high selective pressure to a limited set of isoforms for neural wiring. On the other hand, the epitope II is predicted to be involved in heterophilic bindings and possesses a higher sequence diversity, consistent with a secondary function as PRR (Meijers et al. 2007).

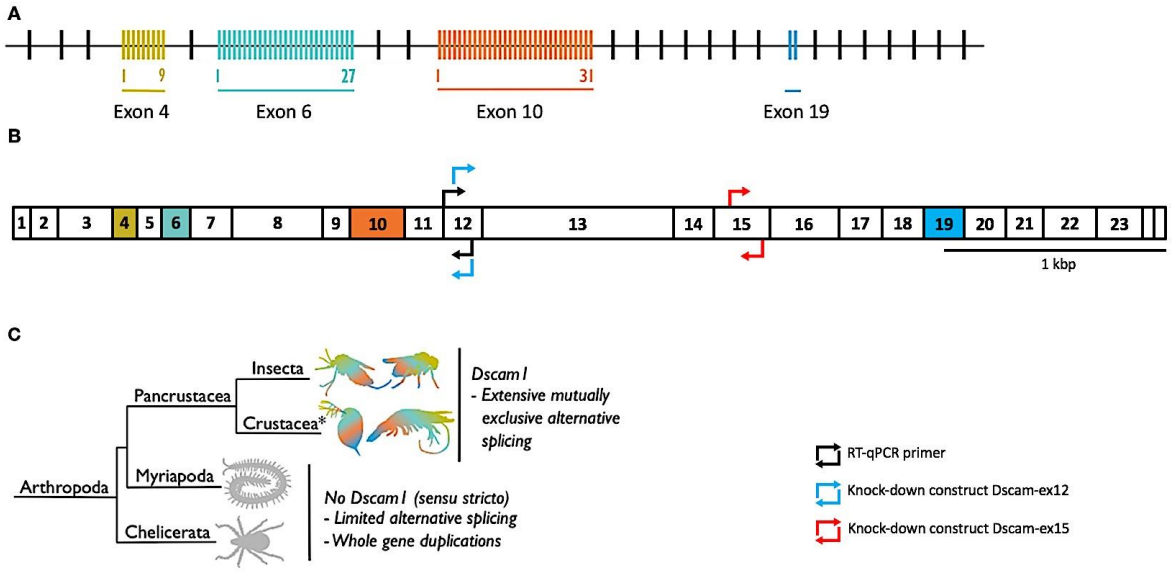

Figure 1.2 - Schematic representation of genomic and mRNA *Dscam1* sequences from *T. castaneum* and known occurrences of *Dscam1* in arthropods. (A) illustrates *T. castaneum Dscam1* gene (accession number: TC012539), while **(B)** represents its mRNA with the corresponding exon numbers. Alternatively spliced regions are coloured. Black arrows indicate the position of the RTqPCR primers for expression analysis. Blue (Dscam-ex12) and red (Dscam-ex15) arrows indicate the position of knock-down constructs for RNAi mediated depletion of *Dscam1* in *T. castaneum*. **(C)** Until now, *Dscam1* has only been found in pancrustaceans. Myriapods and chelicerates have diversified the Dscam gene family through other routes. *Crustacea is considered a paraphyletic group containing the hexapods; phylogeny follows **(Legg et al. 2013)**. Scale indicates 1kbp. Figure adapted from Armitage *et al.* (2017).

1.3.1 Dscam1 in immunity

More recently, *Dscam1* mRNA was found in haemocytes and fat bodies, immune cells of pancrustaceans (Neves et al. 2004; Watson et al. 2005), as well as the secreted tail-less Dscam1 protein in the haemolymph (Watson et al. 2005). Through microarrays it was estimated that these immune cells can produce up to ~ 18,000 receptor isoforms of Dscam1 in *Drosophila*. The splice variants found in haemocytes and fat bodies differ from the ones found in the brain (Watson et al. 2005). In *T. castaneum*, 69 variable exons (Figure 1.2A) can give rise to 15,066 different Dscam1 isoforms (Armitage & Brites 2016) . It was proposed that due to their hypervariability, they could have a role as PRR and therefore in immunity (Boehm 2007; Watson et al. 2005).

In the past decade, several studies have been showing a relation between Dscam1 and immunity. For instance, flies with *Dscam1* knock-down haemocytes are unable to efficiently phagocytose bacteria compared to the control flies (Watson et al. 2005). In crayfish, *Dscam1* was found to be induced in haemocytes upon contact to MAMPs like lipopolysaccharides and b-1, 3-glucans (Li et al. 2015). It was reported that different Dscam1 isoforms bind to a different degree to *Escherichia coli*, suggesting a possible role as specific opsonin (Watson et al. 2005). Furthermore, infection of *A. gambiae* individuals with different parasites induced the expression of different Dscam1 splice isoforms (Dong et al. 2006). Recently Fu and colleagues have shown (Fu et al. 2014) in primed *Litopenaeus vannamei* that a knock-down of *Dscam1* leads to a decrease in the phagocytosis of the white spot syndrome virus (WSSV) upon secondary infection. Consequently, the groups treated with Dscam1-siRNA injections showed a lower survival compared to the control-siRNA groups. Although, this last study concerns virus infection, it is the first study showing a direct effect of Dscam1 in immune priming (Armitage et al. 2015). In contrast, a study with the shrimp *Artemia fransciscana* did not observe any significant difference in *Dscam1* expression during TGIP, either within the generation challenged with *Vibrio campbellii* or its offspring (Norouzitallab et al. 2016).

Studies (Brites et al. 2011; Chávez-Galarza et al. 2013) have shown that *Dscam1* may be under balancing selection. It is known that genes involved in pathogen recognition, such as the major histocompatibility complex, tend to show long-term balancing selection (Takahata et al. 1992; Ferrer-Admetlla et al. 2008).

Dscam1 intracellular diversity also originates from exon inclusion/exclusion and type III polyadenylation (Chou et al. 2011; Yu et al. 2009). These may result in different protein products being produced (Lutz & Moreira 2011). Therefore, the same locus may be able to generate both tail-less and membrane-bound forms (Chou et al. 2011). Different combinations of Dscam1 transmembrane and cytoplasmic domains variants may explain how the receptor is able to be involved in different systems and in response to specific stimulus activate distinct signal transduction pathways inside each one of them (Yu et al. 2009).

In shrimp, upon infection with WSSV there is an increase in both tail-less and transmembrane Dscam1 (Chiang et al. 2013). Moreover, when facing a natural pathogen as the bacterium *Vibrio harveyi*, Dscam1 isoforms show a more specific and stronger pattern response. In the latter, there was a particular up-regulation of alternative tail-less variants that contain an immune-related endocytosis/phagocytosis motif (Hung et al. 2013). Parallel to this, there is an up-regulation of the splicing activator B52 and down-regulation of the splicing repressor Hrp36. This expression changes may lead to the increased production of membrane-bound and tail-less Dscam found in shrimp after WSSV infection (Chiang et al. 2013). In addition, IMD and Toll pathway are thought to mediate species-specific defences in *A. gambiae* infected with *Plasmodium* and bacteria. The latter is possible through the transcriptional regulation of the splicing factors Caper and IRSF1 that leads to the production of pathogen-specific splice variants of *Dscam1* (Dong et al. 2012).

Regarding the secreted form of Dscam1, it was first hypothesized to be produced through proteolytic cleavage of the membrane-bound Dscam1 (Watson et al. 2005). In shrimp, several alternative stop codons were found inside the *Dscam1* gene (Ng et al. 2014) reinforcing the hypothesis that tail-less Dscam may be produced directly through type III polyadenylation (Chou et al. 2009). Its hypothesized role may be also similar to adaptive immunity elements. Soluble Dscam1 binds to *Escherichia coli* (Watson et al. 2005) and was found in the *D. melanogaster* phagosome proteome (Stuart et al. 2007). Additionally, its epitope configuration hypothetically allows a Dscam1 isoform to form a homodimer that through the hypervariable epitope II may be capable of recognition and opsonisation of pathogens (Meijers et al. 2007; Stuart & Ezekowitz 2008). Studies have already shown specificity on the isoform production upon pathogen infection (Dong et al. 2006; Hung et al. 2013; Chiang et al. 2013).

Over the last years, some studies have been positioning Dscam1 as an important element in bacteria regulation. In 2006, Dong and colleagues (Dong et al. 2006) showed in *A. gambiae* that after *Dscam1* knock-down, there was a reduction in the phagocytosis index and the bacteria in the haemolymph proliferated. Through sequence analyses of the bacterial *16S rRNA*, they were able to relate them with three Gram-negative bacteria species. In addition, an increased number of *Plasmodium* oocysts on the midgut were found. Six years later, the same group overexpressed different Dscam1 forms naturally induced by *Plasmodium* and bacteria. Curiously, they observed that the bacteria-induced form (exon 4.14) led to a reduction in the amount of midgut bacteria in comparison to the control and *Plasmodium*-induced forms of Dscam1 (Dong et al. 2012). It is known that Dscam1 is expressed in haemocytes (Watson et al. 2005), cells capable of phagocytosis. Phagocytosis should be dependent on MAMPs recognition by PRRs. If in fact *Dscam1* is responsible for a large PRR repertoire, then a knock-down may preclude the identification and therefore the regulation of the microbiota.

In contrast, Zhang (Zhang et al. 2016) has shown opposite results for the influence of Dscam1 on extracellular bacteria. In the latter, *Laodelphax striatellus* with a knock-down of *Dscam1* showed a decrease in the infection of both rice strip virus and *Wolbachia* compared to the control. However, no change was observed in the number of extracellular bacteria (Zhang et al. 2016). It is possible that Dscam1 may have an intracellular role and its knock-down may have disrupted the intracellular environment, making it less suitable for intracellular parasites.

In short, invertebrates' complex microbial communities appear to be interconnected with the host's immunity and occasionally even operate as an extension of it (Sommer & Bäckhed 2013). A rich microbiota seems to be decisive not only for basal immunity but also for specific mechanisms, such as immune priming (Futo et al. 2015). Dscam1 may play a crucial role in pancrustacean immunity as a PRR, opsonin and regulator of bacterial microbiota, contributing to the host homeostasis (Boehm 2007; Watson et al. 2005; Dong et al. 2006).

1.4 Aim of the thesis

The overall aim of this thesis is to understand the role of Dscam1 in the whole-body bacterial microbiota of *T. castaneum*. It has been suggested that Dscam1 may have a role in pancrustacean immune recognition (Boehm 2007) and might be essential to the regulation of bacterial microbiota (Dong et al. 2006). However, there is contradictory evidence for the latter function (Dong et al. 2006; Dong et al. 2012; Zhang et al. 2016). Therefore, I aim to clarify if Dscam1 regulates bacterial microbiota in *T. castaneum* by knocking down *Dscam1* and quantify the total amount of bacteria throughout *T. castaneum* development.

2. Materials and Methods

2.1 Model organism: *Tribolium castaneum*

Insects are the most diverse group of animals on Earth and represent more than half of the living species known to Mankind. Insects strong interactions with microbes allow the dissection of immune reactions that are easily overlooked in vertebrate systems (Chambers & Schneider 2012) and may influence the immune outcome of infections and diseases in higher vertebrates as the human (Mukherjee et al. 2015).

Coleoptera is the most evolutionary successful order of animals, covering the majority of the habitats (Hunt et al. 2007). *Tribolium castaneum* (Herbst 1797), a member of Coleoptera, is a severe agricultural pest that has shown resistance to all classes of insecticides used against it (Richards et al. 2008). It is an important model organism in ecology and evolution and has allowed the development of a vast range of concepts, such as the competition theory (Park 1962). This beetle presents advantages such ease of culture, short generation time, high fecundity and the availability of several genetic tools, such as genetic markers (Demuth et al. 2007). As in *Caenorhabditis elegans*, RNA interference (RNAi) is systemic in *Tribolium*, allowing knock-down of specific gene products in any developmental point (Tomoyasu & Denell 2004). Moreover, its genome was recently sequenced facilitating genetic studies with the organism (Richards et al. 2008). Additionally, T. castaneum possess a hypervariable *Dscam1* capable of producing 15.066 different isoforms (Watson et al. 2005). This organism also exhibits a dynamic microbiota across development. Actinobacteria, Bacteroidetes, Firmicutes and Proteobacteria are the predominant phyla found in this organism and their proportion changes across developmental stages (Futo 2016).

T. castaneum Cro 1 population established from 165 beetle pairs wild collected in Croatia in 2010 (Milutinović et al. 2013), was used in the following experiments. As a food source and substrate, organic wheat flour with 5% brewer's yeast was used, which prior to use was frozen at -20°C and then heated up to room temperature (~20°C). The population was kept under controlled conditions: 30ºC, 70% humidity and on a 12-hour light-dark cycle (Bucher 2009).

2.2 Time-point experiment hypothesis and preliminary tests

Studies have shown that contradictory results for *Dscam1* role as bacteria regulator in the gut and haemolymph (Dong et al. 2006; Dong et al. 2012; Zhang et al. 2016). Therefore, the aim of the main experiment was to clarify Dscam1 role in *T. castaneum* microbiota across its development, through *Dscam1* knock-down. The bacterial *16S rRNA* was used as a proxy for the total amount of whole-body bacteria in the beetle. Three developmental time-points were analyzed: 15-days old larvae, 23-days-old pupae and 30-days old adults. Prior to the start of this experiment, several questions had to be answered to assure the methodology was optimized. The several points are described below.

2.2.1 Is it possible to detect expression for all genes in RTqPCR using Power Microbiome™ RNA isolation kit?

A previous study from Futo *et al.* **(2015)** used the Power Microbiome RNA isolation kit (MO BIO Laboratories, Inc.) for RNA extraction, since it performed better in the bacterial *16S rRNA* extraction from the beetle. However, earlier tests shown *Dscam1* may present low expression. Therefore, it was important to test if we could get a reliable signal from all genes in study using this particular RNA extraction kit. In this study were used as reference gene for the amount of beetle RNA, the *ribosomal protein 49* (*Rp49*) and the *ribosomal protein L13a* (*Rpl13a*). As target genes were used the bacterial *16S rRNA* and *Dscam1*. *Rp49* and *Rpl13a* are used as reference genes for the amount of beetle RNA in the experiment.

For this, we analysed the following three beetle developmental stages: ~15-days old individuals (larval stage), ~25 days-old individuals (pupal stage) and ~35 days-old individuals (adult stage). Each developmental stage was composed by three replicates of 10 pooled individuals. The animals were separated through the use of 280µm and 710µm sieve and their age was estimated by separation through the sieves and size of the individuals. Directly after the separation, they were frozen in liquid nitrogen and stored at -80ºC. The RNA was then extracted with the Power Microbiome™ RNA isolation kit (MO BIO Laboratories, Inc.) under sterile conditions. RNA concentration and absorbance ratios were measured with Qubit® and Implen Nanophotometer®. A reverse transcription of 500ng of RNA was performed with Superscript III kit (Invitrogen™) to 20µl of final volume of cDNA. Afterwards, a RTqPCR for all four genes at the different developmental stages was performed on a 96-well plate using the following protocol: pre-incubation at 95ºC for 3 minutes followed by 40 cycles of 10 seconds at 95ºC, 20s at 58ºC and 2s at 72ºC. The fluorescence acquisition was performed in each cycle at 72ºC. In order to confirm the identity of the PCR products, a melting curve was derived using the temperature range between 95 and58ºC, as in Futo *et al.* **(2015)**. A control with water instead of cDNA was used as a control for the sterility of the RTqPCR solutions. Detailed protocols and list of primers used can be found in the section 6.1 and 6.4 of the appendices, respectively. Primers position in the mRNA are illustrated in Figure 1.2B.

2.2.2 Does microbiota-enriched food increase the amount of bacteria detectable via RTqPCR?

We hypothesized that if beetles were raised on flour enriched with microorganisms that they would develop an increased bacterial load, which might be beneficial in the case that *Dscam1* knock-down reduces the bacterial microbiota. To test this hypothesis, two different media were prepared: i) microbiota-enriched-media, where 100 adults and 100 larvae were placed in 100g of flour with 5% yeast for 3 days before the oviposition, adapted from Futo *et al.* **(2015)**; and ii) regular-media, only flour with 5% yeast without any exposure to larvae or adults. A ~2000 individuals' subpopulation of approximately 1-month old adults were then allowed to oviposit in the two flours types for 24 hours. On the eleventh day after oviposition larvae were transferred to a 96-well plate to simulate the main experiment conditions. Three different stages were analysed: larvae (15-days old), pupae (23-days old) and adults (30-days old). For each combinatorial treatment (developmental stage x media), 3 biological replicates of 10 pooled individuals were considered. RNA extraction, reverse transcription and RTqPCR for *16S rRNA* and *rp49* was performed as the previous experiment. The larval samples did not contain 500ng of RNA, so these samples reverse transcription was performed with only 100ng of RNA.

2.2.3 Does individuals' surface sterilization affect levels of bacterial 16S rRNA detected via RTqPCR?

Previous analysis of the bacterial *16S rRNA* expression were performed without any type of surface sterilization of the individual before RNA extraction. Therefore, it was unknown to us if we were mostly detecting external or internal bacterial *16S rRNA* expression. Considering we are particularly interested in the gut and haemolymph microbiota because it is the bacteria that presumably would be affected by *Dscam1* knock-down, it was important to test if the surface microbiota was large enough to camouflage any *Dscam1* knock-down effect on internal microbiota. To access this question, we performed larvae sterilization in order to see if there is any reduction in the expression levels of *16S rRNA* and *Dscam1*. If bacteria on the external insect cuticle represents a significant proportion of the total bacteria, we predict that we would see a weaker *16S rRN*A signal after surface sterilization compared to the controls.

In this study, one sterilization treatment and two control treatments took place. The sterilization treatment was submitted to the following methodology, adapted from Futo *et al.* (2015). Larvae (~15-days old) were separated from the flour with a 710µm sieve and subjected to 20 minutes on ice for anaesthetic purposes. After this, three replicates of 10 pooled larvae were positioned between two nets and submerged for 20 seconds in each of the following solutions: Ethanol 70%, MilliQ-water, sodium hypoclorite (NaClO) at 2% and two final washes in MilliQ-water. This process was performed separately for each sample group of 10 pooled larvae and solutions were changed between each one. Directly afterwards, they were frozen in liquid nitrogen and stored at -80°C until the next day, when the RNA extraction took place for all the treatments. Two controls treatments took place: Control and Ice. The Control treatment used the same methodology as the rest of the above-described experiments, i.e., the larvae were directly frozen, while larvae in the Ice treatment were placed for 20 minutes on ice before being frozen in liquid nitrogen. The latter was used to see if there was any effect from the anaesthesia on ice on gene expression. RNA extraction, reverse transcription and RTqPCR for bacterial *16S rRNA*, *Dscam1* and *rp49* was performed as above.

2.2.4 Do both dsRNA constructs result in a successful Dscam1 knock-down on 11-days old larvae?

In order to proceed to the main experiment, it was important to assure we could get an effective *Dscam1* knock-down in 11-days old larvae. For this, two different dsRNA constructs were used to knock-down *Dscam1*. Exon 12 and 15 regions were selected for RNAi mediated knock-down because both are non-alternatively spliced regions within the *T. castaneum Dscam1* gene (Peuß et al. 2016) (Figure 1.2B). A region of the *Escherichia coli* gene *aspargine synthetas*e (Nakamura et al. 1981) (*asnA*) that is not found in *T. castaneum*, was used as a control for the dsRNA machinery. This control was named RNAi treatment. Injections with phosphate-buffered saline (PBS) were performed in one of the treatments as a control for the injection itself. A last group of animals that were not subjected to any type of injection was added as control in the experiment and was named naive treatment. The dsRNA injections were performed on 11-days old larvae. Two different dsRNA concentrations were tested: ~2600 ng/µl and ~1700 ng/µl.

Thus, eight treatments took place:

1) Dscam-ex12+, knock-down for *Dscam1* exon 12 at the concentration of ~2600ng/µl;
2) Dscam-ex12-, knock-down for *Dscam1* exon 12 at the concentration of ~1700ng/µl;
3) Dscam-ex15+, knock-down for *Dscam1* exon 15 at the concentration of ~2600ng/µl;

4) Dscam-ex15-, knock-down for *Dscam1* exon 15 at the concentration of ~1700ng/µl;
5) RNAi+, *asnA* at the concentration of ~2600ng/µl;
6) RNAi-, *asnA* at the concentration of ~1700ng/µl;
7) PBS;
8) Naive.

For each treatment, whole-body samples from 3 biological replicates of 10 pooled individuals were considered. Injections took place between the 1st and 2nd integument with a glass capillary and without the usage of carbon dioxide or any other chemical for anesthetic purposes. Directly afterwards, they were individualized in a 96-well plate with flour and 5% yeast, posteriorly taped and ~8 holes per well were made to allow for air exchange. Each 96-well plate had an equal number of individuals from each treatment randomly distributed through the plate. The order of the injections was also performed randomly. Injections were performed in 3 blocks in consecutive days.

The plates were then incubated at 30ºC, 70% humidity and on a 12-hour light-dark cycle for four days. After the four days, survival for each group was quantified and the larvae were frozen in liquid nitrogen and stored at -80ºC. The RNA extraction, reverse transcription and RTqPCR for all four genes (*rp49*, *rpl13a*, *Dscam1* and bacterial *16S rRNA*) was performed as in the previous experiments. A 1.5% TBE agarose gels were performed to assess dsRNA and RNA quality prior to injections and prior to reverse transcription, respectively.

2.3 Effect of *Dscam1* knock-down on *Tribolium castaneum* microbiota dynamics

As described before, the intention of this experiment is to clarify the role of Dscam1 in the microbiota dynamics of *T. castaneum*, through the knock-down of *Dscam1*. Hence, three developmental stages were analysed: Larval (15-days old); pupal (23-days old); and adult stage (30-days old). Five injection treatments took place:

1) Dscam-ex12, knock-down for *Dscam1* exon 12;
2) Dscam-ex15, knock-down for *Dscam1* exon 15;
3) RNAi, control for dsRNA machinery activation using *asnA* gene;
4) PBS, control for the injection itself;
5) Naive, individuals not subjected to any kind of injection.

The concentration of dsRNA used was ~1700ng/µl. For each combinatorial treatment (developmental stage x injection treatment) 5 replicates of 10 pooled individuals were considered. Injections were performed in 5 blocks in consecutive days. Both injections and individualization in the 96-well plate were performed as in the preliminary test on the *Dscam1* knock-down.

The plates were then incubated at 30ºC, 70% humidity and on a 12-hour light-dark cycle for four days. A block of injections was randomly removed from the incubator 4, 12 and 19 days after the injections for larval, pupal and adult stage analysis. For pupal and adult samples, each replicate had 5 females and 5 males. RNA extraction, reverse transcription and RTqPCR for bacterial *16S rRNA*, *Dscam1*, *rp49* and *rpl13a* was performed as above. Each RTqPCR plate had a common sample obtained from a unique RT, working as a control for variation between plates. A 1.5% TBE agarose gels were performed to assess dsRNA and RNA quality prior to injections and prior to reverse transcription, respectively.

2.4 Data analysis and software

2.4.1 RTqPCR data

The data obtained from the RTqPCR assays was analysed through the Ct comparative method (Schmittgen & Livak 2008). In this project, the Ct value was defined as the crossing point qPCR cycle. Absolute gene expression was presented as 2^{-Ct}, whereas relative gene expression was given as below:

$$Relative\ expression = 2^{-\Delta Ct} = 2^{-(Ct\ gene\ of\ interest - Ct\ reference\ gene)}$$

A geometric mean of the different replicates 2^{-C} or $2^{-\Delta Ct}$ was calculated for each treatment, as well as the correspondent standard error. Hence, a higher 2^{-Ct} corresponds to a higher expression from the gene in analysis, while a higher $2^{-\Delta Ct}$ correlates with a higher expression of the gene of the interest comparatively to the reference gene(s).

The fold change in expression due to the *Dscam1* knock-downs was calculated as below:

$$Fold\ change = 2^{-\Delta\Delta Ct}$$
$$= 2^{-[(Ct\ gene\ of\ interest - Ct\ reference\ gene)_{Treated} - (Ct\ gene\ of\ interest - Ct\ reference\ gene)_{Control}}$$

The knock-down treated groups were compared to the RNAi control group. Since, the fold change due to the knock-downs represents a reduction in the gene expression, the inverse of the fold change was calculated in the sections below.

2.4.2 Statistical analysis

The expression of the reference genes *rp49* and *rpl13a* was used to normalise the expression of the target genes *Dscam1* and bacterial *16S rRNA*. The several statistical tests/models were performed on the 2^{-Ct} /$2^{-\Delta Ct}$ expression values using the software RStudio (Version 1.0.143) (Team 2015).

Additionally, the data obtained from RTqPCR for comparisons between treated and untreated samples was analysed with REST2009 Software (Qiagen GmbH). This software calculations are based on the model by Pfaffl (Pfaffl et al. 2002). The program determines whether there is a significant difference in the expression of target genes comparatively to the expression of reference genes between treated and untreated samples. The program takes in account the different reaction efficiencies of both reference and target genes.

3. Results and Discussion

3.1 Preliminary tests

3.1.1 Detection of gene expression through RTqPCR

The aim of this preliminary test was to confirm that we could get a reliable signal from all the four genes used in the main experiment when using RNA extracted with the Power Microbiome™ RNA isolation kit. The Ct values for each of the four genes, is described in the Table 3.1. In general, the reference genes *Rp49* and *Rpl13a* were detectable at earlier cycle numbers, which is expected from genes coding for widely-expressed ribosomal proteins (Cardoso et al. 2014; Scharlaken et al. 2008). On the other hand, *Dscam1* presents a later cycle number signal, possibly due to its limited and specific expression in certain beetle tissues (Watson et al. 2005; Neves et al. 2004). Lastly, the bacterial *16S rRNA* presents a rather early average signal for a bacterial gene. The RNA isolation kit used is optimized to extract bacterial RNA (Futo et al. 2015) and that could explain its early cycle number when compared to beetle genes. Since we obtained reliable signals from all the genes, we continued the experiments using this RNA isolation kit.

Table 3.1 – RTqPCR Ct values at which *Rp49*, *Rpl13a*, *Dscam1* and bacterial *16S rRNA* expression were detected across the three beetle developmental stages. Each sample is composed of 10 pooled individuals.

	Rp49	***Rpl13a***	***Dscam1***	***16S rRNA***
Larvae	~22	~25	~27	~25
Pupae	~23	~25	~26	~25
Adults	~22	~27	~28	~27

3.1.2 Does microbiota-enriched food increase the amount of bacteria detectable via RTqPCR?

Dscam1 may have a positive effect (Zhang et al. 2016) on symbionts. In this case, a knock-down of *Dscam1* would presumably lead to their reduction. A strong reduction in the whole-body bacteria might not be observed in the RTqPCR. Therefore, it was important to test if it would be possible to increase the beetle bacterial load detectable in the RTqPCR in case there is a strong reduction in the bacteria after *Dscam1* knock-down in the main experiment. For this, individuals grown in regular flour were compared to individuals grown in a microbiota-enriched flour and their bacterial *16S rRNA* expression was analysed for differences in three developmental stages: larval, pupal and adult stage.

In this experiment, we did not observe any significant difference in *Rp49* expression across treatments (Kruskal-Wallis: p-value = 0.2752). Since the qPCR signal for larval samples only appeared after the cycle 35, they were removed from the analysis. This result may be due to the lack of RNA in these samples for cDNA reverse-transcription and consequently RTqPCR. Concerning the adult and pupal samples, no significant difference was observed in the bacterial *16S rRNA* relative expression between individuals grown on regular flour and grown on microbiota-enriched flour

(REST, pupae: p-value=0.643; adults: p-value=0.226) (Figure 3.1). These results suggest there is no effect of the microbiota-enriched media on the bacterial load of the individuals in the pupal and adult stage. It is possible that the individuals in the regular flour already possess a large bacterial load and an increase is not possible even if there are more microorganisms available in the media.

Nonetheless, we cannot discard other hypotheses. It is possible that the microbiota-enriched media does not possess more microorganisms than the regular flour. Prior to the oviposition in these media, larvae and adults were left living on the flour. These individuals may have consumed a significant part of the flour resources and their microorganisms. Therefore, in the end there might be no difference between the two types of flour. To test this hypothesis, we would have to quantify the bacteria in both flours. An optimum experimental scenario would be to add directly the microorganisms to the flour and then compare the individuals that lived on either one of them. However, this was not possible to perform and we do not know if that would affect the results in the main experiment.

Hence, taking the results obtained from the pupal and adult stage, the hypothesis that a microbiota-enriched flour could increase the bacterial load observed in a RTqPCR was refuted. Therefore, we proceeded to the main experiment using regular flour.

3.1.3 Does surface sterilization affect levels of bacterial 16S rRNA detected via RTqPCR?

The aim of this experiment was to test if the bacteria in the cuticle that is not affected by the knock-down of *Dscam1* would camouflage any effect caused by the knock-down on the internal microbiota. For this purpose, a Sterilization treatment and two controls took place. While the individuals of the Sterilization treatment were anesthetized on ice and posteriorly sterilized, the individuals of the Ice treatment were only subjected to the anaesthesia on ice. The Control treatment was not treated at all.

Regarding this experiment, there is no significant difference in the reference gene *rp49* across treatments (Kruskall- Wallis: p-value = 0.1479). For each biological replicate, *Dscam1* and *16S rRNA* relative expression to the reference gene *rp49* was calculated and plotted (Figure 3.2). Both Ice and Sterilization treatment were compared to the Control treatment through the use of REST software.

The relative expression of the bacterial *16S rRNA* in Ice and Sterilization treatment did not differ from the Control treatment (REST, Ice: p-value = 0.508; Sterilization: p-value = 0.666). At least two hypotheses can explain this result. The first is that the surface sterilization methodology used may not have worked. In this scenario, *16S rRNA* expression would naturally not differ between treatments. Although we cannot discard the possibility that this type of sterilization may not work on *T. castaneum* larval cuticle, given the extensive literature on successful surface sterilization of arthropods through similar methods (Dong et al. 2006; Montagna et al. 2015; Chandler et al. 2011) we are more inclined to the second and following hypothesis. It is possible that the methodology used has been able to remove the majority or total amount of bacteria in the beetle cuticle but this quantity is too low compared to the bacteria found inside of the beetle. Moreover, the RTqPCR using *16S rRNA* may not provide enough discriminatory power to observe small-scale changes in the total amount of bacteria. Also, the bacterial load on and inside the beetle is not standardized and it may present a wide variation across individuals what by itself can overshadow fine differences between treatments.

In the case of *Dscam1*, differences were observed across treatments. According to REST statistics, there is a significant difference between both treatments with anaesthesia on ice and the control non-treated on ice: Ice (REST, p-value = 0,005) and Sterilization (REST, p-value = 0,017).

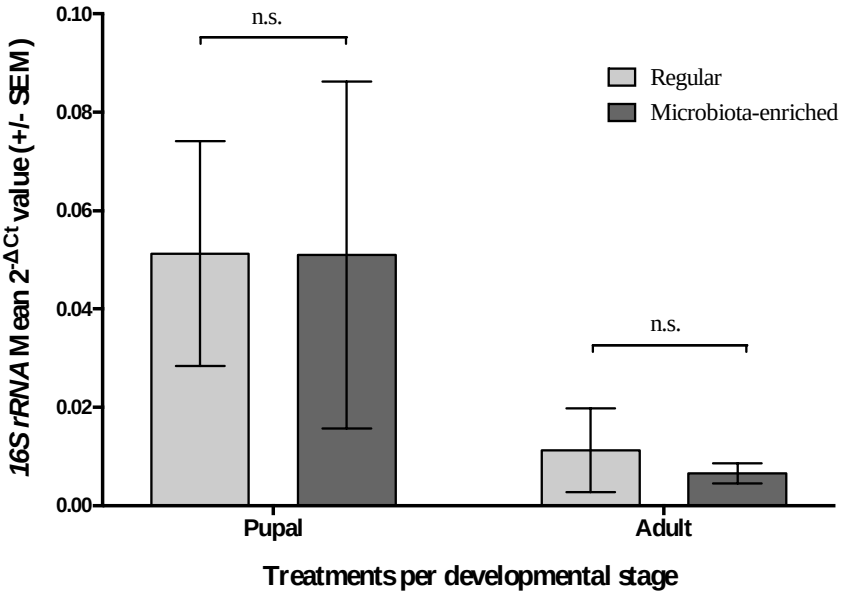

Figure 3.1 – Mean $2^{-\Delta Ct}$ values from RTqPCR for bacterial *16S rRNA* expression across microbiota-enriched flour and regular flour treatments in pupal and adult stage. A higher $2^{-\Delta Ct}$ value corresponds to a higher expression from 16S rRNA compared to the reference gene *rp49*. For each treatment 3 biological replicates of 10 pooled individuals were used. Two different media treatments were prepared and compared: i) Microbiota-enriched-media, where 100 adults and 100 larvae were placed in 100g of flour with 5% yeast for 3 days before the oviposition as in (Futo et al. 2015); and ii) Regular-media, only flour with 5% yeast without any previous preparation. The graphs show group mean plus/minus standard error of the mean. n.s. stands for not significant.

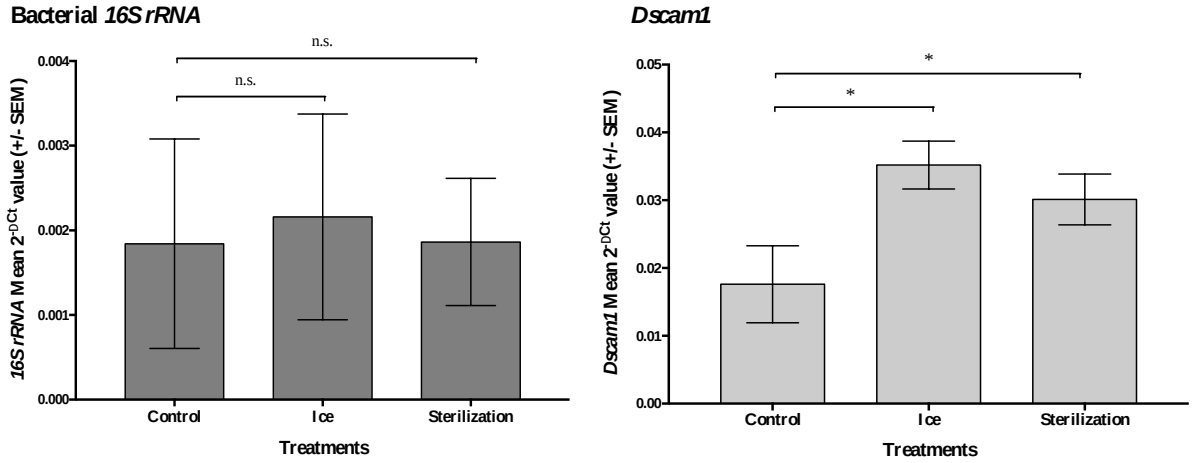

Figure 3.2 – Relative expression of the bacterial *16S rRNA* and *Dscam1* across a surface sterilization treatment and two control treatments. For each treatment 3 biological replicas of 10 pooled larvae were used. Three treatments are shown: Control, where the larvae were directly frozen in liquid nitrogen; Ice, where the larvae were submitted to 20 minutes on ice; and Sterilization, where the larvae were put on ice for 20 minutes for anesthetic purposes and after 20 seconds in Ethanol 70%, MilliQ-water, Sodium hypochlorite at 2% and two washes in MilliQ-water, sequentially. The graphs show group mean plus standard error of the mean. Not significant differences through REST statistics are represented with n.s., while significant are illustrated with a *.

This might be explained by an upregulation caused by the cold shock. This effect has been shown in some genes in *Drosophila* (Goto 2001; Colinet et al. 2010). Nonetheless, compared to the literature mentioned before, the individuals were only subjected to a relatively short period of time to cold temperatures and then directly frozen. This short period of time might not be long enough to induce the *Dscam1* upregulation and explain our result.

Due to the lack of difference in *16S rRNA* expression and the effect of the cold treatment on *Dscam1*, we decided to proceed to the main experiment without sterilization of the individuals.

3.1.4 Do both dsRNA constructs result in a successful Dscam1 knock-down after dsRNA injection on 11-days old larvae?

Before advancing to the main experiment it was important to confirm that we could achieve a *Dscam1* knock-down after dsRNA injection on 11-day old larvae. The results from this test are described below.

In terms of larval survival 4 days after injection (Figure 6.1), we observe that the dsRNA treatments show a low survival compared to PBS (injection control) and Naive (non-treated individuals) controls. Overall the higher concentration of dsRNA (~2600ng/µl) leads to a 5% higher mortality than the lower dsRNA concentration (~1700ng/µl). This may be easily explained by the physical constraints upon injection, such as higher viscosity of the solution leading to a higher damage. *Dscam1* knock-down treatments are the ones that show lower survival with the average ranging from 52% to 60%. In comparison, the RNAi control treatments show slightly better survival values (66 and 70%). This slight difference may be due to collateral effects of the knock-down on the larval metabolism and motility (Peuß et al. 2016). Concerning PBS, a much higher survival is observed (around 86%). The slight mortality in this last treatment is most likely due to the aggressive and inherent effect of the injection on a reduced larval size at this age. Naive individuals show a 98% survival; the small mortality can be explained by the handling on such a young age.

Regarding *Dscam1* relative expression, we compared the values from all treatments to the RNAi control (Figure 3.3). This comparison allows a more accurate differentiation between the effects from the dsRNA against *Dscam1* and possible effects from dsRNA machinery activation or the injection itself on the target gene expression. It has been observed that PBS injection is enough to strongly alter the expression of some genes in *T. castaneum* (Behrens et al. 2014).

Although an average half-reduction in *Dscam1* expression is observed across all the knock-down treatments, only the Dscam-ex12- treatment is significantly different from the RNAi- control (REST, p-value < 0.001). In this treatment, the knock-down resulted in a 63% *Dscam1* down-regulation, similar to what earlier studies (Peuß et al. 2016) achieved with the same construct in same age *T. castaneum* larvae. The lack of significance is most likely explained by the strong variation on the relative expression of *Dscam1* throughout the treatments. Moreover, it seems there is a weaker knock-down when using higher dsRNA concentrations. A higher dsRNA concentration results in a higher viscosity of the solution that may have a larger impact on the larval metabolism and may interfere with the correct dsRNA processing, leading to a less pronounced knock-down.

In comparison to the PBS and Naive controls, the RNAi control seems to also suffer a *Dscam1* down-regulation. This down-regulation may be caused by secondary effects of the dsRNA machinery activation, since it is not observed on the injection control.

Taking into account these results, we decided to proceed to the main experiment with only the lower dsRNA concentration (~1700ng/µl) since it results in an effective knock-down and slight higher

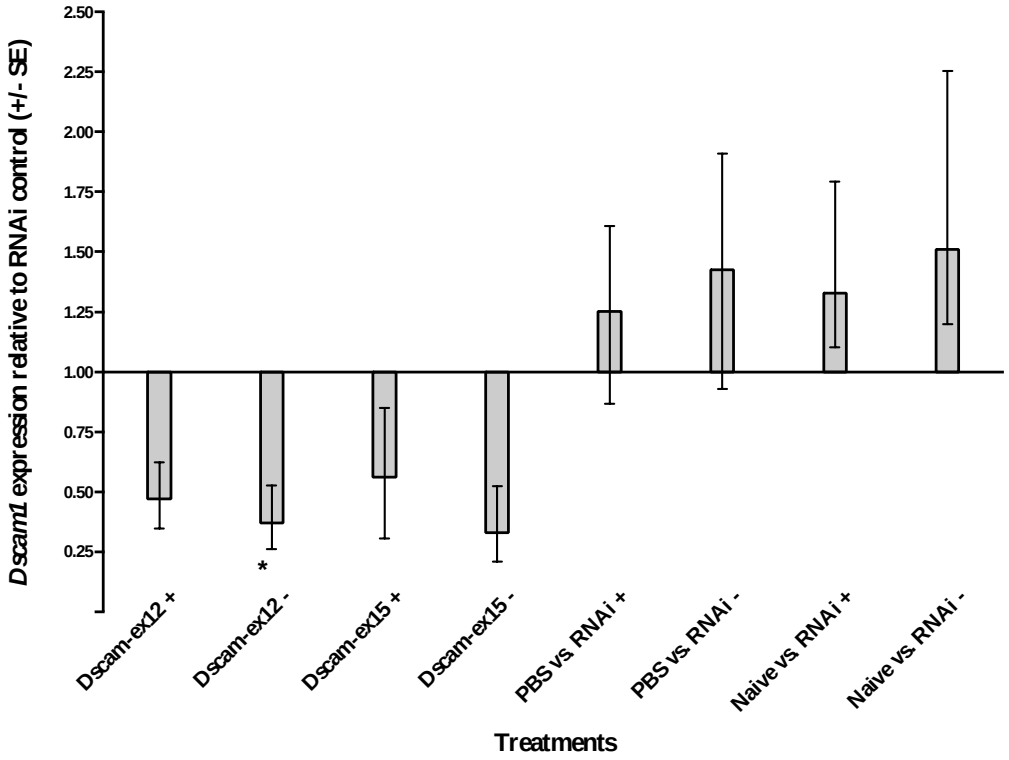

Figure 3.3 - Expression of *Dscam1* relative to the RNAi control after injection of *Dscam1* dsRNA. Each treatment is composed by whole-body samples from 3 replicates of ten 15-day old larvae. Injections took place in 11-day old larvae. Two different dsRNA concentrations were tested: ~2600ng/µl and ~1700ng/µl. Higher dsRNA concentration knock-down treatments (Dscam-ex12+ and Dscam-ex15+) were compared to a high dsRNA concentration RNAi control (RNAi+). In the same way, the lower dsRNA concentration treatments (Dscam-ex12- and Dscam-ex15-) were compared to a low dsRNA concentration RNAi control (RNAi-). The expression of the reference genes *rp49* and *rpl13a* was used to normalise the expression of the *Dscam1*. Although there is an overall reduction in *Dscam1* expression in knock-down treatments, only Dscam-ex12- was significantly different from the control. Means and standard errors were calculated with the REST software. Significant differences through REST software are represented with a *.

larval survival compared to the higher concentration. In addition, the larval survival was considered in the planning of number of individuals to be injected in the main experiment.

3.2 Effect of *Dscam1* knock-down on *Tribolium castaneum* microbiota dynamics

Since both the trial (Section 3.1.4) and this experiment were performed under identical conditions, the data were combined for the larval time-point. A larval replicate was removed from the data-set since it did not meet the requirements for analysis. Therefore, all the results presented below are based on 7 pools of 10 individuals for the larval time-point and 5 pools of 10 individuals for pupal and adult time-points.

There was no statistically significant variation in the reference genes across treatments or developmental time-points. Regarding *Dscam1*, its expression varies according to treatments (p-value < 0.0001) and developmental time-points (p-value <0.0001). The latter was already reported in a previous study in *T. castaneum* (Peuß et al. 2016). In all time-points a significant knock-down in both Dscam-ex12 and Dscam-ex15 treatments was observed when compared to the RNAi control. The knock-down treatments led to a reduction of at least 55% of *Dscam1* expression in all time-points (Table 6.4).

Concerning, the bacterial *16S rRNA* expression, there is no significant difference between knock-down treatments and RNAi control according to REST statistics (Figure 3.4). These results suggest Dscam1 is not involved in the bacterial regulation in *T. castaneum*, similar observations by Zhang *et al.* (2016). A possible explanation would be that the system is robust enough to function with low *Dscam1* levels. Several pathways in the immune system work in redundancy to assure the system works even if one of the pathways is deficient. The non-significance might also be explained by the high variation and reduced number of replicates. As we can observe in Figure 3.5, there are relatively high values of *Dscam1* even in knock-down treatments. This lack of consistency in some samples might explain why there is no significant effect on the microbiota. The *Dscam1* knock-down treatments in the adult time-point show the higher value of *16S rRNA* for any treatment at any time-point. It is possible that the *Dscam1* knock-down is no longer strong enough to interfere with bacterial regulation, not allowing the observation of a statistically significant increase in the bacterial load. Other possible explanation for the high values at this time-point concerns the unknown Dscam1 half-life. It is conceivable that both transmembrane and secreted form of the protein only decreased in a later time-point, such as the adult time-point. Therefore, a change in the bacterial load would only be observed when a required amount of Dscam1 would not be reached, leading to an unbalance of the bacterial microbiota in the beetle.

The Box-Cox transformed relative expression of the bacterial *16S rRNA* was also analysed in a linear model (ANOVA type II) using treatment and developmental time-point as independent factors and Box-Cox transformed *Dscam1* as a continuous predictor variable. The model included two-way interactions between developmental time-point and treatment, and developmental time-point and *Dscam1* expression, as well as the main effects. The interaction was statistically significant with *Dscam1* expression (p-value < 0.0001) but not with the developmental time-point (p-value = 0.26112) and treatment (p-value = 0.38296). The non-significant interaction between *16S rRNA* and treatment is in agreement with the statistics from REST above. Nevertheless, there is a strong interaction between *16S rRNA* and *Dscam1* expression. Subsequently, we plotted the relative expression of *16S rRNA* against the relative expression of *Dscam1* (Figure 3.5) and compared them by a Spearman's rank correlation test. As expected, there is a statistically significant negative correlation between the relative expression of *16S rRNA* and *Dscam1* for the larval (p-value = 0.03918, ρ = -0.3564553) and adult time-point (p-value = 0.01403, ρ = -0.489230) but not for the pupal time-point (p-value = 0.261, ρ = -0.2330769). If the data from all three time-points were combined, the correlation remains significant (p-value= 0.002088, ρ = -0.3327326). Overall, a higher expression of *Dscam1* is linked to a lower *16S rRNA* expression and therefore lower bacterial load. This tendency is identical to the one described by Dong and colleagues (2006;2012). The correlation seems to be stronger in the adult time-point. The fact that there is not a significant correlation in the pupal time-point may be due to the increase in the *Dscam1* expression levels as a consequence of the neuronal rewiring upon the beetle metamorphosis. This increase in the neural circuits would cloud any correlation or effect linked to an immune phenomenon and/or bacterial regulation during the pupal stage.

Hence, it seems the *Dscam1* knock-down does not affect the bacterial load in the beetle. It is possible that the RTqPCR primers used in this study do not amplify some groups of bacteria that might have been affected by the treatment. However, previous microbiota analysis with this and several others suggest that possibility is very unlikely. Although it is merely speculative, it is conceivable that Dscam1 may only have a role on a specific stage of development. In the adult time-point we observed both higher *16S rRNA* expression levels and correlation coefficient between the genes. This might be an indication of some event or function for *Dscam1* in this stage. The only two studies that reported an increase in the

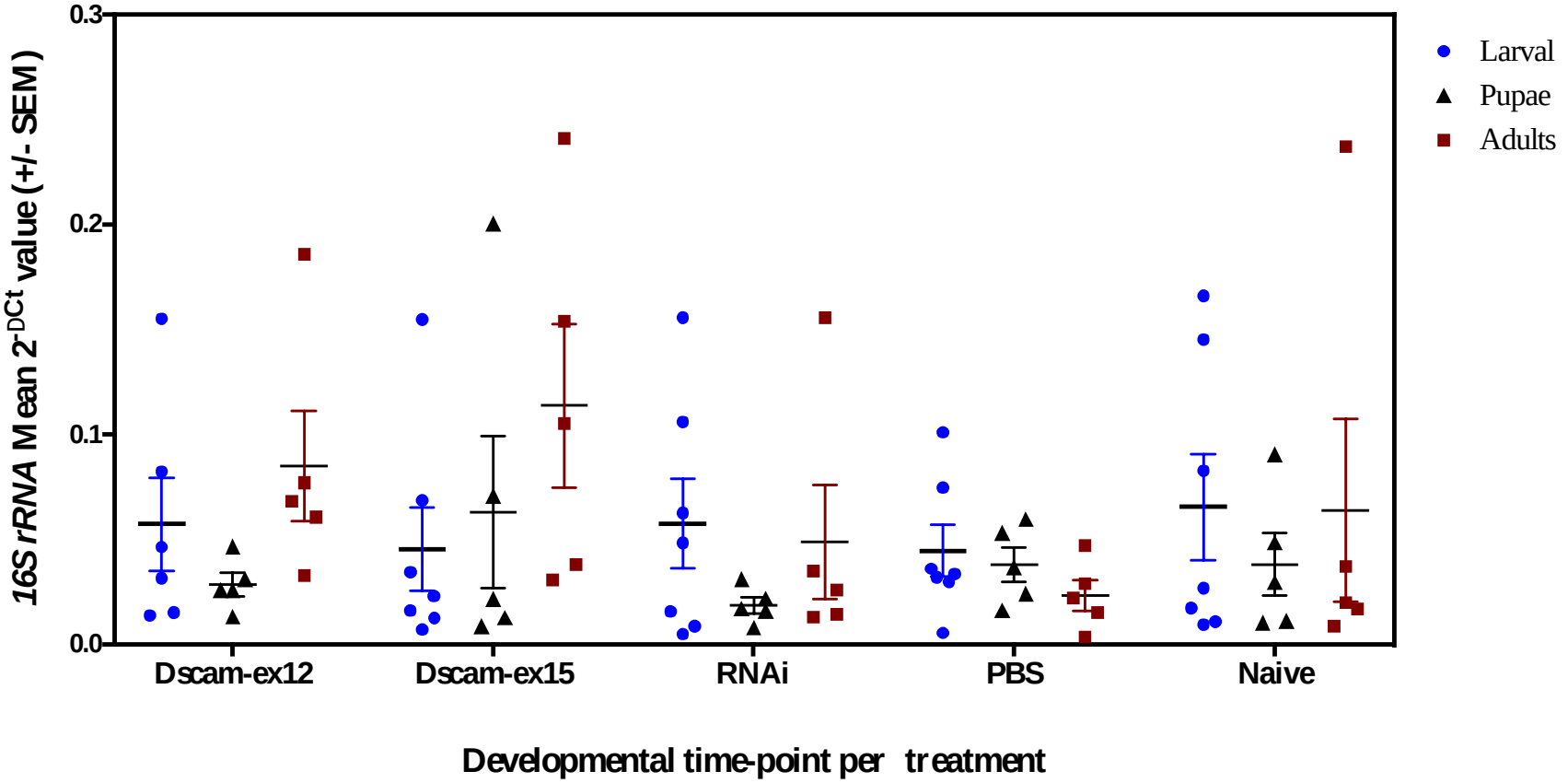

Figure 3.4 - Relative expression of the bacterial *16S rRNA* across developmental time-points and treatments. Five treatments are represented: 2 knock-down treatments (Dscam-ex12 and Dscam-ex15), RNAi control, PBS control and Naive control. Three different developmental time-points were analysed for each treatment: 15-days old larvae (n=7), 23-days old pupae (n=5) and 30-days old adult (n=5). There is no significant difference in the bacterial *16S rRNA* expression across treatments and therefore no effect of *Dscam1* knock-down on the bacterial load in *T.* castaneum. The graphs show group mean plus standard error of the mean.

in the bacterial load after *Dscam1* knock-down were both conducted in adult mosquitoes (Dong et al. 2006; Dong et al. 2012). On the other hand, Zhang and colleagues (2016) who did not observe any change in the bacterial load after Dscam1 knock-down performed the analysis in third-instar nymphs, before the metamorphosis to the adult stage. The fact that the knock-down is reduced in this time-point may not allow us to conclude if this might be a specific stage regulation.

Furthermore, we do not possess information about bacterial composition. If Dscam1 has a recognition and/or regulatory function, it is also likely to lead to shifts in the proportion of different classes of bacteria and not necessarily changes in the total amount of bacteria. By what we known about immunity, it is unlikely for a receptor system to explain recognition of all microbes. Then, the knock-down may affect the regulation of a certain classes of bacteria. The reduction in regulation would lead to an increase in those classes that would compete with the rest of the bacteria in the same environment. Though hypothetical, it is possible that *Dscam1* knock-down may have triggered an unbalance in the bacterial microbiota at some level. A deeper analysis at the bacterial microbiota composition would shed light on this hypothesis and potentially link Dscam1 with the recognition/regulation of some bacterial classes in *T. castaneum*.

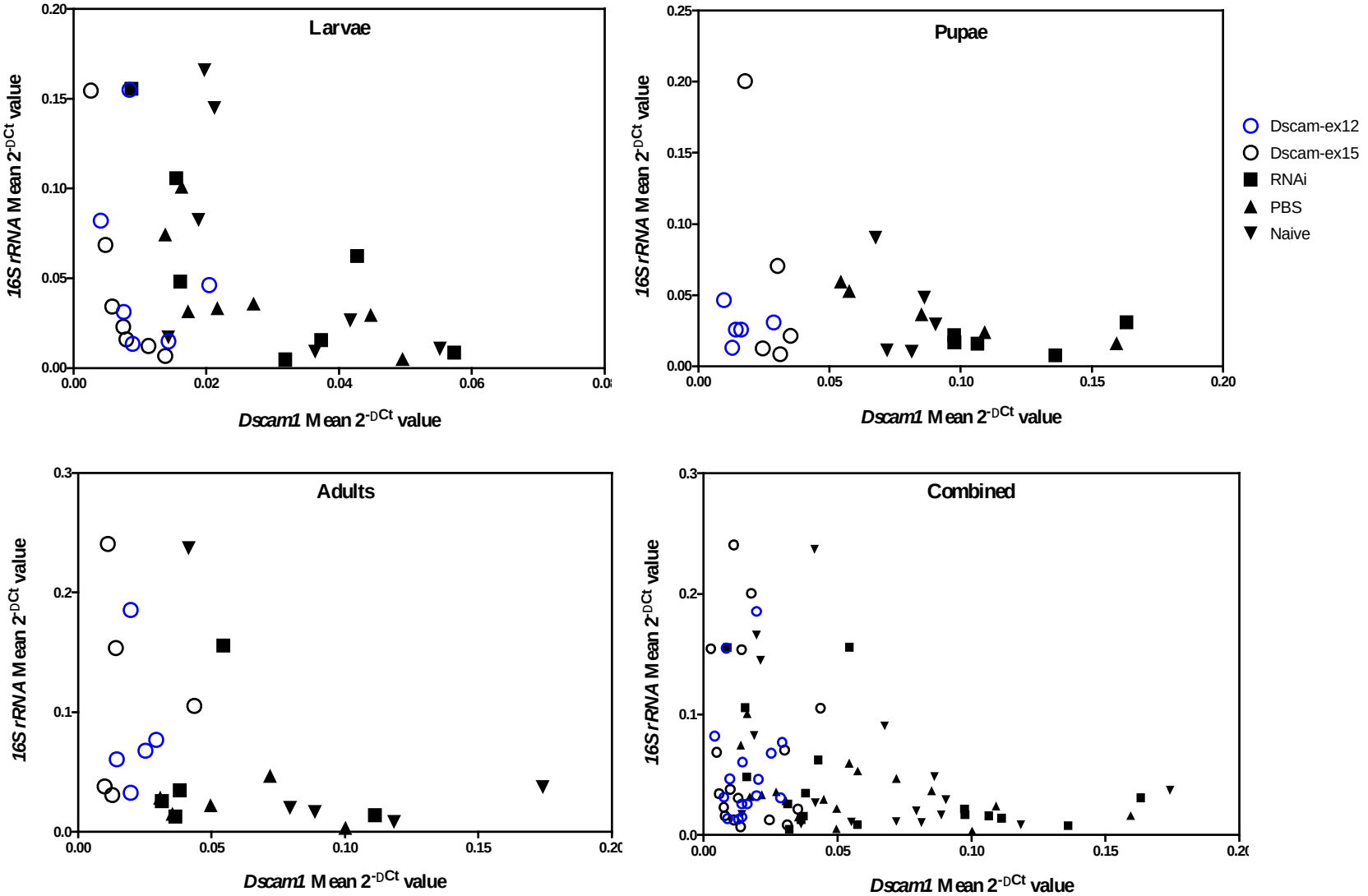

Figure 3.5 – Relative expression of the bacterial *16S rRNA* against relative expression of *Dscam1*. The five treatments' genes expression are individually represented by time-point and all combined. A negative correlation was observed in the larval and adult time-points, as well as in the combined data (Spearman: *larvae* p-value = 0.03918, ρ = -0.3564553; *pupae* p-value = 0.261, ρ = -0.2330769; *adults* p-value = 0.01403, ρ = -0.489230; *combined* p-value = 0.002088, ρ = -0.3327326). The data suggests that a higher value for Dscam1 is correlated with a lower value for the bacterial *16S rRNA*.

4. Concluding remarks

The results from this study show no evidence for an effect of a *Dscam1* knock-down on the bacterial load of *T. castaneum* at three developmental time-points: 15-days old larvae, 23-days old pupae and 30-days old adults. Although not significant, an increase in the bacterial load in the adult time-point was observed. At this time-point the *Dscam1* knock-down had already been reduced and it is possible that is the reason why we did not observe an effect in the bacterial microbiota, in comparison to other studies. Nevertheless, we observed a strong correlation between the relative expression of *Dscam1* and relative expression of the bacterial *16S rRNA* at the larval and adult time-point. Our data suggests *Dscam1* may be involved in immunity and in particular with the regulation of the microbiome. Nonetheless, its role still remains unclear. We cannot discard a function as a PRR and/or bacterial regulator for *Dscam1* since we do not have information concerning bacterial composition after *Dscam1* knock-down.

In future studies, it would be interesting to analyse the bacterial composition after *Dscam1* knock-down. If this molecule possesses a function as PRR/bacterial regulator, then its reduction would lead to an increase of the classes of bacteria negatively regulated by Dscam1 and potentially a reduction in the proportion of other bacterial classes caused by competition.

It would also be important to analyse and characterize the beetle microbiota and its dynamics at several time-points in each of the developmental stages. As an example, this study could help clarify the concept of core microbiota. A characterization of the beetle microbiota could also work as basis and reference panel for future studies concerning microbiota analysis, such as this one or the bacterial composition analysis described above.

In order to clarify *Dscam1* role in immunity, it would be important to elucidate for how long both transmembrane and secreted proteins persist in the haemolymph. Knowledge regarding *Dscam1* and its relation with microbiota is crucial for the understanding of the evolution of immunity and immune priming in invertebrates.

5. References

Armitage, S.A.O. et al., 2012. The evolution of Dscam genes across the arthropods. *BMC evolutionary biology*, 12(1), p.53.

Armitage, S.A.O. & Brites, D., 2016. The Immune-Related Roles and the Evolutionary History of Dscam in Arthropods. *The Evolution of the Immune System: Conservation and Diversification*, p.241.

Armitage, S.A.O., Peuss, R. & Kurtz, J., 2015. Dscam and pancrustacean immune memory–a review of the evidence. *Developmental & Comparative Immunology*, 48(2), pp.315–323.

Behrens, S. et al., 2014. Infection routes matter in population-specific responses of the red flour beetle to the entomopathogen Bacillus thuringiensis. *BMC genomics*, 15(1), p.1.

Boehm, T., 2007. Two in one: dual function of an invertebrate antigen receptor. *Nature immunology*, 8(10), pp.1031–1033.

Bosch, T.C.G., 2014. Rethinking the role of immunity: lessons from Hydra. *Trends in immunology*, 35(10), pp.495–502.

Brites, D. et al., 2013. More than one way to produce protein diversity: duplication and limited alternative splicing of an adhesion molecule gene in basal arthropods. *Evolution*, 67(10), pp.2999–3011.

Brites, D. et al., 2011. Population genetics of duplicated alternatively spliced exons of the Dscam gene in Daphnia and Drosophila. *PLoS One*, 6(12), p.e27947.

Brucker, R.M. & Bordenstein, S.R., 2012. The roles of host evolutionary relationships (genus: Nasonia) and development in structuring microbial communities. *Evolution*, 66(2), pp.349–362.

Bucher, G., 2009. The beetle book. *Published online by the author. URL: www. gwdg. de/~ gbucher1/tribolium-castaneum-beetle-book1. pdf*.

Cardoso, G.A. et al., 2014. Selection and validation of reference genes for functional studies in the Calliphoridae family. *Journal of Insect Science*, 14(1), p.2.

Cerenius, L. & Söderhäll, K., 2004. The prophenoloxidase-activating system in invertebrates. *Immunological reviews*, 198(1), pp.116–126.

Chambers, M.C. & Schneider, D.S., 2012. Pioneering immunology: insect style. *Current opinion in immunology*, 24(1), pp.10–14.

Chandler, J.A. et al., 2011. Bacterial communities of diverse Drosophila species: ecological context of a host–microbe model system. *PLoS Genet*, 7(9), p.e1002272.

Chávez-Galarza, J. et al., 2013. Signatures of selection in the Iberian honey bee (Apis mellifera iberiensis) revealed by a genome scan analysis of single nucleotide polymorphisms. *Molecular ecology*, 22(23), pp.5890–5907.

Chiang, Y.-A. et al., 2013. Shrimp Dscam and its cytoplasmic tail splicing activator serine/arginine (SR)-rich protein B52 were both induced after white spot syndrome virus challenge. *Fish & shellfish immunology*, 34(1), pp.209–219.

Chou, P.-H. et al., 2011. Penaeus monodon Dscam (PmDscam) has a highly diverse cytoplasmic tail and is the first membrane-bound shrimp Dscam to be reported. *Fish & shellfish immunology*,

30(4), pp.1109–1123.

Chou, P.-H. et al., 2009. The putative invertebrate adaptive immune protein Litopenaeus vannamei Dscam (LvDscam) is the first reported Dscam to lack a transmembrane domain and cytoplasmic tail. *Developmental & Comparative Immunology*, 33(12), pp.1258–1267.

Colinet, H., Lee, S.F. & Hoffmann, A., 2010. Temporal expression of heat shock genes during cold stress and recovery from chill coma in adult Drosophila melanogaster. *The FEBS journal*, 277(1), pp.174–185.

Contreras-Garduño, J. et al., 2016. Insect immune priming: ecology and experimental evidences. *Ecological Entomology*.

Corby-Harris, V. et al., 2007. Geographical distribution and diversity of bacteria associated with natural populations of Drosophila melanogaster. *Applied and environmental microbiology*, 73(11), pp.3470–3479.

Delabar, J.M. et al., 1992. Molecular mapping of twenty-four features of Down syndrome on chromosome 21. *European journal of human genetics: EJHG*, 1(2), pp.114–124.

Demuth, J.P. et al., 2007. Genome-wide survey of Tribolium castaneum microsatellites and description of 509 polymorphic markers. *Molecular Ecology Notes*, 7(6), pp.1189–1195.

Dishaw, L.J. et al., 2014. The gut of geographically disparate Ciona intestinalis harbors a core microbiota. *PLoS One*, 9(4), p.e93386.

Dong, Y. et al., 2012. Anopheles NF-κB-regulated splicing factors direct pathogen-specific repertoires of the hypervariable pattern recognition receptor AgDscam. *Cell host & microbe*, 12(4), pp.521–530.

Dong, Y., Manfredini, F. & Dimopoulos, G., 2009. Implication of the mosquito midgut microbiota in the defense against malaria parasites. *PLoS pathogens*, 5(5), p.e1000423.

Dong, Y., Taylor, H.E. & Dimopoulos, G., 2006. AgDscam, a hypervariable immunoglobulin domain-containing receptor of the Anopheles gambiae innate immune system. *PLoS Biol*, 4(7), p.e229.

Dybdahl, M.F. & Lively, C.M., 1998. Host-parasite coevolution: evidence for rare advantage and time-lagged selection in a natural population. *Evolution*, pp.1057–1066.

Eggert, H., Kurtz, J. & Diddens-de Buhr, M.F., 2014. Different effects of paternal trans-generational immune priming on survival and immunity in step and genetic offspring. In *Proc. R. Soc. B*. The Royal Society, p. 20142089.

Engel, P. & Moran, N.A., 2013. The gut microbiota of insects–diversity in structure and function. *FEMS microbiology reviews*, 37(5), pp.699–735.

Ferrer-Admetlla, A. et al., 2008. Balancing selection is the main force shaping the evolution of innate immunity genes. *The Journal of Immunology*, 181(2), pp.1315–1322.

Franzenburg, S. et al., 2013. Distinct antimicrobial peptide expression determines host species-specific bacterial associations. *Proceedings of the National Academy of Sciences*, 110(39), pp.E3730–E3738.

Fraune, S. & Bosch, T.C.G., 2007. Long-term maintenance of species-specific bacterial microbiota in the basal metazoan Hydra. *Proceedings of the National Academy of Sciences*, 104(32), pp.13146–13151.

Fu, L., Li, T. & Wang, Y., 2014. Potential role of LvDscam in specific immune response of

Litopenaeus vannamei against white spot syndrome virus by oral delivery of VP28 using Bacillus subtilis. *Aquaculture Research*.

Fuerst, P.G. et al., 2009. DSCAM and DSCAML1 function in self-avoidance in multiple cell types in the developing mouse retina. *Neuron*, 64(4), pp.484–497.

Futo, M., 2016. *The role of microbes as mediators of immune memory in insects*. Westfälische Wilhelms-Universität Münster.

Futo, M., Armitage, S.A.O. & Kurtz, J., 2015. Microbiota plays a role in oral immune priming in Tribolium castaneum. *Frontiers in microbiology*, 6.

Goto, S.G., 2001. A novel gene that is up-regulated during recovery from cold shock in Drosophilamelanogaster. *Gene*, 270(1), pp.259–264.

Greenwood, J.M. et al., 2017. Oral immune priming with Bacillus thuringiensis induces a shift in the gene expression of Tribolium castaneum larvae. *BMC genomics*, 18(1), p.329.

Hammer, T.J., McMillan, W.O. & Fierer, N., 2014. Metamorphosis of a butterfly-associated bacterial community. *PLoS One*, 9(1), p.e86995.

Hanshew, A.S. et al., 2013. Minimization of chloroplast contamination in 16S rRNA gene pyrosequencing of insect herbivore bacterial communities. *Journal of microbiological methods*, 95(2), pp.149–155.

Hattori, D. et al., 2008. Dscam-mediated cell recognition regulates neural circuit formation. *Annual review of cell and developmental biology*, 24, pp.597–620.

Hattori, D. et al., 2007. Dscam diversity is essential for neuronal wiring and self-recognition. *Nature*, 449(7159), pp.223–227.

Hillyer, J.F., 2016. Insect immunology and hematopoiesis. *Developmental & Comparative Immunology*, 58, pp.102–118.

Hiramoto, M. et al., 2000. The Drosophila Netrin receptor Frazzled guides axons by controlling Netrin distribution. *Nature*, 406(6798), pp.886–889.

Hooper, L. V & Gordon, J.I., 2001. Commensal host-bacterial relationships in the gut. *Science*, 292(5519), pp.1115–1118.

Hornef, M.W. et al., 2002. Bacterial strategies for overcoming host innate and adaptive immune responses. *Nature immunology*, 3(11), pp.1033–1040.

Hughes, M.E. et al., 2007. Homophilic Dscam interactions control complex dendrite morphogenesis. *Neuron*, 54(3), pp.417–427.

Hung, H.-Y. et al., 2013. Properties of Litopenaeus vannamei Dscam (LvDscam) isoforms related to specific pathogen recognition. *Fish & shellfish immunology*, 35(4), pp.1272–1281.

Hunt, T. et al., 2007. A comprehensive phylogeny of beetles reveals the evolutionary origins of a superradiation. *Science*, 318(5858), pp.1913–1916.

Kaufman, J., 2010. Evolution and immunity. *Immunology*, 130(4), pp.459–462.

Koch, H. & Schmid-Hempel, P., 2012. Gut microbiota instead of host genotype drive the specificity in the interaction of a natural host-parasite system. *Ecology letters*, 15(10), pp.1095–1103.

Koropatnick, T.A. et al., 2004. Microbial factor-mediated development in a host-bacterial mutualism. *Science*, 306(5699), pp.1186–1188.

Kurtz, J., 2005. Specific memory within innate immune systems. *Trends in immunology*, 26(4), pp.186–192.

Kurtz, J. & Franz, K., 2003. Innate defence: evidence for memory in invertebrate immunity. *Nature*, 425(6953), pp.37–38.

Lavine, M.D. & Strand, M.R., 2002. Insect hemocytes and their role in immunity. *Insect biochemistry and molecular biology*, 32(10), pp.1295–1309.

Lawrence Zipursky, S. & Grueber, W.B., 2013. The molecular basis of self-avoidance. *Annual review of neuroscience*, 36, pp.547–568.

Lazzaro, B.P. & Rolff, J., 2011. Danger, microbes, and homeostasis. *Science*, 332(6025), pp.43–44.

Lederberg, J. & McCray, A.T., 2001. Ome SweetOmics--A Genealogical Treasury of Words. *The Scientist*, 15(7), p.8.

Lee, Y.K. & Mazmanian, S.K., 2010. Has the microbiota played a critical role in the evolution of the adaptive immune system? *Science*, 330(6012), pp.1768–1773.

Leger, A.J.S. et al., 2017. An Ocular Commensal Protects against Corneal Infection by Driving an Interleukin-17 Response from Mucosal γδ T Cells. *Immunity*.

Legg, D.A., Sutton, M.D. & Edgecombe, G.D., 2013. Arthropod fossil data increase congruence of morphological and molecular phylogenies. *Nature communications*, 4.

Lemaitre, B. & Hoffmann, J., 2007. The host defense of Drosophila melanogaster. *Annu. Rev. Immunol.*, 25, pp.697–743.

Li, D. et al., 2015. Antimicrobial activity of a novel hypervariable immunoglobulin domain-containing receptor Dscam in Cherax quadricarinatus. *Fish & shellfish immunology*, 47(2), pp.766–776.

Little, T.J. & Kraaijeveld, A.R., 2004. Ecological and evolutionary implications of immunological priming in invertebrates. *Trends in Ecology & Evolution*, 19(2), pp.58–60.

Lutz, C.S. & Moreira, A., 2011. Alternative mRNA polyadenylation in eukaryotes: an effective regulator of gene expression. *Wiley Interdisciplinary Reviews: RNA*, 2(1), pp.22–31.

Makarova, O. et al., 2016. Antimicrobial defence and persistent infection in insects revisited. *Phil. Trans. R. Soc. B*, 371(1695), p.20150296.

Marmaras, V.J. & Lampropoulou, M., 2009. Regulators and signalling in insect haemocyte immunity. *Cellular signalling*, 21(2), pp.186–195.

Matthews, B.J. & Grueber, W.B., 2011. Dscam1-mediated self-avoidance counters netrin-dependent targeting of dendrites in Drosophila. *Current Biology*, 21(17), pp.1480–1487.

Mazmanian, S.K. et al., 2005. An immunomodulatory molecule of symbiotic bacteria directs maturation of the host immune system. *Cell*, 122(1), pp.107–118.

Medzhitov, R. & Janeway, C.A., 1997. Innate immunity: the virtues of a nonclonal system of recognition. *Cell*, 91(3), pp.295–298.

Meijers, R. et al., 2007. Structural basis of Dscam isoform specificity. *Nature*, 449(7161), pp.487–491.

Milutinović, B. et al., 2016. Immune priming in arthropods: an update focusing on the red flour beetle. *Zoology*.

Milutinović, B., Fritzlar, S. & Kurtz, J., 2013. Increased survival in the red flour beetle after oral

priming with bacteria-conditioned media. *Journal of innate immunity*, 6(3), pp.306–314.

Montagna, M. et al., 2015. Metamicrobiomics in herbivore beetles of the genus Cryptocephalus (Chrysomelidae): toward the understanding of ecological determinants in insect symbiosis. *Insect science*, 22(3), pp.340–352.

Mukherjee, K., Twyman, R.M. & Vilcinskas, A., 2015. Insects as models to study the epigenetic basis of disease. *Progress in biophysics and molecular biology*, 118(1), pp.69–78.

Mylonakis, E. et al., 2016. Diversity, evolution and medical applications of insect antimicrobial peptides. *Phil. Trans. R. Soc. B*, 371(1695), p.20150290.

Nakamura, M. et al., 1981. Nucleotide sequence of the asnA gene coding for asparagine synthetase of E. coli K-12. *Nucleic acids research*, 9(18), pp.4669–4676.

Neves, G. et al., 2004. Stochastic yet biased expression of multiple Dscam splice variants by individual cells. *Nature genetics*, 36(3), pp.240–246.

Ng, T.H. et al., 2014. Review of Dscam-mediated immunity in shrimp and other arthropods. *Developmental & Comparative Immunology*, 46(2), pp.129–138.

Norouzitallab, P. et al., 2016. Probing the phenomenon of trained immunity in invertebrates during a transgenerational study, using brine shrimp Artemia as a model system. *Scientific reports*, 6.

Obbard, D.J. et al., 2009. Quantifying adaptive evolution in the Drosophila immune system. *PLoS Genet*, 5(10), p.e1000698.

Ochman, H. et al., 2010. Evolutionary relationships of wild hominids recapitulated by gut microbial communities. *PLoS biology*, 8(11), p.e1000546.

Park, T., 1962. Beetles, competition, and populations. *Science*, 138(3548), pp.1369–1375.

Paust, S. & Von Andrian, U.H., 2011. Natural killer cell memory. *Nature immunology*, 12(6), pp.500–508.

Peuß, R. et al., 2016. Down syndrome cell adhesion molecule 1: testing for a role in insect immunity, behaviour and reproduction. *Royal Society open science*, 3(4), p.160138.

Pfaffl, M.W., Horgan, G.W. & Dempfle, L., 2002. Relative expression software tool (REST©) for group-wise comparison and statistical analysis of relative expression results in real-time PCR. *Nucleic acids research*, 30(9), pp.e36–e36.

Richards, S. et al., 2008. The genome of the model beetle and pest Tribolium castaneum. *Nature*, 452(7190), pp.949–955.

Rodrigues, J. et al., 2010. Hemocyte differentiation mediates innate immune memory in Anopheles gambiae mosquitoes. *Science*, 329(5997), pp.1353–1355.

Roth, O. et al., 2010. Paternally derived immune priming for offspring in the red flour beetle, Tribolium castaneum. *Journal of Animal Ecology*, 79(2), pp.403–413.

Ryu, J.-H. et al., 2008. Innate immune homeostasis by the homeobox gene caudal and commensal-gut mutualism in Drosophila. *science*, 319(5864), pp.777–782.

Scharlaken, B. et al., 2008. Reference gene selection for insect expression studies using quantitative real-time PCR: The head of the honeybee, Apis mellifera, after a bacterial challenge. *Journal of insect Science*, 8(33), pp.1–10.

Schmid-Hempel, P., 2005. Evolutionary ecology of insect immune defenses. *Annu. Rev. Entomol.*, 50,

pp.529–551.

Schmittgen, T.D. & Livak, K.J., 2008. Analyzing real-time PCR data by the comparative CT method. *Nature protocols*, 3(6), pp.1101–1108.

Schmucker, D. et al., 2000. Drosophila Dscam is an axon guidance receptor exhibiting extraordinary molecular diversity. *Cell*, 101(6), pp.671–684.

Schmucker, D. & Chen, B., 2009. Dscam and DSCAM: complex genes in simple animals, complex animals yet simple genes. *Genes & development*, 23(2), pp.147–156.

Sharon, G. et al., 2010. Commensal bacteria play a role in mating preference of Drosophila melanogaster. *Proceedings of the National Academy of Sciences*, 107(46), pp.20051–20056.

Siva-Jothy, M.T., Moret, Y. & Rolff, J., 2005. Insect immunity: an evolutionary ecology perspective. *Advances in insect physiology*, 32, pp.1–48.

Sommer, F. & Bäckhed, F., 2013. The gut microbiota—masters of host development and physiology. *Nature Reviews Microbiology*, 11(4), pp.227–238.

Spoel, S.H. & Dong, X., 2012. How do plants achieve immunity? Defence without specialized immune cells. *Nature Reviews Immunology*, 12(2), pp.89–100.

Stuart, L.M. et al., 2007. A systems biology analysis of the Drosophila phagosome. *Nature*, 445(7123), pp.95–101.

Stuart, L.M. & Ezekowitz, R.A., 2008. Phagocytosis and comparative innate immunity: learning on the fly. *Nature Reviews Immunology*, 8(2), pp.131–141.

Takahata, N., Satta, Y. & Klein, J., 1992. Polymorphism and balancing selection at major histocompatibility complex loci. *Genetics*, 130(4), pp.925–938.

Team, Rs., 2015. RStudio: integrated development for R. *RStudio, Inc., Boston, MA URL http://www. rstudio. com*.

Teixeira, L., Ferreira, Á. & Ashburner, M., 2008. The bacterial symbiont Wolbachia induces resistance to RNA viral infections in Drosophila melanogaster. *PLoS Biol*, 6(12), p.e1000002.

Thongaram, T. et al., 2005. Comparison of bacterial communities in the alkaline gut segment among various species of higher termites. *Extremophiles*, 9(3), pp.229–238.

Tomoyasu, Y. & Denell, R.E., 2004. Larval RNAi in Tribolium (Coleoptera) for analyzing adult development. *Development genes and evolution*, 214(11), pp.575–578.

Trauer-Kizilelma, U. & Hilker, M., 2015. Impact of transgenerational immune priming on the defence of insect eggs against parasitism. *Developmental & Comparative Immunology*, 51(1), pp.126–133.

Turnbaugh, P.J. et al., 2007. The human microbiome project: exploring the microbial part of ourselves in a changing world. *Nature*, 449(7164), p.804.

Van Valen, L., 1973. A new evolutionary law. *Evolutionary theory*, 1, pp.1–30.

Watson, F.L. et al., 2005. Extensive diversity of Ig-superfamily proteins in the immune system of insects. *Science*, 309(5742), pp.1874–1878.

Weiss, B.L. et al., 2013. Trypanosome infection establishment in the tsetse fly gut is influenced by microbiome-regulated host immune barriers. *PLoS Pathog*, 9(4), p.e1003318.

Winnebeck, E.C., Millar, C.D. & Warman, G.R., 2010. Why does insect RNA look degraded? *Journal of Insect Science*, 10(159), pp.1–7.

Wong, A.C.N., Chaston, J.M. & Douglas, A.E., 2013. The inconstant gut microbiota of Drosophila species revealed by 16S rRNA gene analysis. *The ISME journal*, 7(10), pp.1922–1932.

Woolhouse, M.E.J. et al., 2002. Biological and biomedical implications of the co-evolution of pathogens and their hosts. *Nature genetics*, 32(4), pp.569–577.

Yamakawa, K. et al., 1998. DSCAM: a novel member of the immunoglobulin superfamily maps in a Down syndrome region and is involved in the development of the nervous system. *Human Molecular Genetics*, 7(2), pp.227–237.

Yokoi, K. et al., 2012. Antimicrobial peptide gene induction, involvement of Toll and IMD pathways and defense against bacteria in the red flour beetle, Tribolium castaneum. *Results in immunology*, 2, pp.72–82.

Yu, H.-H. et al., 2009. Endodomain diversity in the Drosophila Dscam and its roles in neuronal morphogenesis. *Journal of Neuroscience*, 29(6), pp.1904–1914.

Yun, J.-H. et al., 2014. Insect gut bacterial diversity determined by environmental habitat, diet, developmental stage, and phylogeny of host. *Applied and environmental microbiology*, 80(17), pp.5254–5264.

Zanchi, C. et al., 2011. Differential expression and costs between maternally and paternally derived immune priming for offspring in an insect. *Journal of Animal Ecology*, 80(6), pp.1174–1183.

Zasloff, M., 2002. Antimicrobial peptides of multicellular organisms. *nature*, 415(6870), pp.389–395.

Zhang, F. et al., 2016. Roles of the Laodelphax striatellus Down syndrome cell adhesion molecule in Rice stripe virus infection of its insect vector. *Insect molecular biology*.

Zipper, H. et al., 2004. Investigations on DNA intercalation and surface binding by SYBR Green I, its structure determination and methodological implications. *Nucleic acids research*, 32(12), pp.e103–e103.

6. Appendices

6.1 Detailed protocols

6.1.1 RNA extraction

The RNA isolation was performed with the Power Microbiome™ RNA isolation kit (MO Bio Laboratories Inc.) in order to maximize the extraction of bacterial RNA. To reduce contaminations, all the RNA extraction protocol was executed under sterile conditions. All the components are stored at room temperature until use, except DNase I that is stored at -20ºC. Only beetles' whole-body samples were used in this study. All the samples were frozen in liquid nitrogen and stored at -80ºC prior to the RNA extraction.

1. Tubes with the frozen samples are put in liquid nitrogen and one by one are smashed with a pestle in liquid nitrogen.
2. For a clear separation of the nucleic acids from the rest of the samples, add 100µl of phenol:chloroform:isoamy alcohol and vortex for some seconds.
3. Add 650µl of solution PM1 previous warmed at 55ºC for 10 minutes and right after mix briefly in the vortex. The solution PM1 contains a lysis buffer that protects the RNA released into the supernatant
4. Mix them in the vortex for 1 minute.
5. Centrifuge at 13.000g for 1 minute at 20ºC.
6. Transfer the supernatant to a clean 2ml collection tube, provided with the kit.
7. Add 150µl of solution PM2 (Inhibitor removal) and vortex briefly for 10 seconds. Incubate in ice for 5 minutes.
8. Gently shake them and centrifuge at 13.000g for 1 minute at 20ºC.
9. Transfer 640µl of the supernatant to clean 2ml collection tube.
10. Add 650µl of solution PM3 and 650µl of 70% Ethanol. Gently shake for a while. The Solution PM3 contains the binding salts for nucleic acid purification. The 70% Ethanol is used to prevent small RNA species from co-purifying with the mRNA and rRNA.
11. Load 650µl of the mix onto a spin filter provided in the kit. Centrifuge at 13.000g for 1 minute at 20ºC. Discard the flow through and repeat until all the mix has been loaded onto the spin filter. The total nucleic acids are bound to the spin filter by passing it through the membrane using centrifugation.
12. Gently shake the solution PM5 and add 650µl of it to the spin filter and centrifuge at 13.000g for 1 minute at 20ºC. The solution PM5 is an isopropanol containing wash buffer to remove salts from the membrane.
13. Discard the flow through and centrifuge again for 1 minute to remove residual waste.
14. Place the spin filter basket into a clean 2 ml Collection tube
15. Prepare a DNase I Solution by mixing 45µl of Solution PM6 and 5µL of DNase I stock solution. The Solution PM6 is a DNase digestion buffer that will digest the genomic DNA on the column.
16. Add 50µl of the DNase I solution into each tube and incubate at room temperature for 15min.
17. Add 400µl of PM7 solution and centrifuge at 13.000g for 1 minute at 20ºC. The solution PM7 is a DNase I inhibitor.

18. Discard the flow through and add 650µl of solution PM5 and centrifuge at 13.000g for 1 minute at 20ºC.
19. Discard the flow through and add 650µl of solution PM4 and centrifuge at 13.000g for 1 minute at 20ºC. The solution PM4 is 100% ethanol used to desalt the column before the elution step.
20. Discard the flow through and centrifuge at 13.000g for 2 minutes at 20ºC to remove any residual waste.
21. Place the spin filter basket into a clean 2ml collection tube.
22. Add 50-100µl of solution PM8 to the center of the filter membrane and wait for 4 minutes. The solution PM8 is RNase-free water for the RNA solubilization. The quantity of RNase-free water you add depends on how concentrated you want the RNA to be.
23. Centrifuge at 13.000g for 1 minute at 20ºC.
24. Discard the spin filter basket. The RNA can be stored at -80ºC

Kit content:
Solution PM1: Lysis buffer
Solution PM2: Inhibitor removal solution
Solution PM3: Binding salts for the total nucleic acid purification
Solution PM4: 100% Ethanol
Solution PM5: Isopropanol with wash buffer
Solution PM6: DNase digestion buffer
Solution PM7: DNase inhibitor
Solution PM8: RNase-free water
DNase I (RNase-Free)
Spin Filters
2ml Collection tubes
Glass beads Tubes

Solutions preparation prior to the RNA isolation:
DNase I Stock enzyme is previously prepared by adding 300µl of RNase-free water (Solution PM8) to the DNase I lyophilized powder and then mixed gently. The solution can be divided in aliquots of 50µl and stored at -20ºC for long term storage.
Under the laminar flow hood, 50µl of phenol:chloroform:isoamy alcohol can be prepared by adding 25µl phenol, 24µl chloroform and 1µl of isoamy alcohol and then gently mixed with the pipette.

6.1.2 Reverse transcription

The reverse transcription of total RNA to cDNA was performed using the kit SuperScript™ III Reverse Transcriptase (Invitrogen®) under sterile conditions. Prior to the reverse transcription, the RNA samples were stored at -80ºC at the total RNA was measured through the use of the Qubit® and Implen NanoPhotometer®. All the components are stored at -20ºC until use. Below is described the protocol for a final volume of 10µl.

1. Add the following components to a nuclease-free water microcentrifuge tube:
    - 0,5µl Random hexamers primers at 100µM
    - 0,5µl 10nM dNTP mix
    - 500ng of total RNA

- Sterile, distilled water until 6,5µl final solution.

2. Start program: heat mixture to 65ºC for 5 minutes.
3. Incubate on ice for at least 1 minute and no more than 5 minutes.
4. Add the following components to the tube:
   - 2µl 5x First-Strand Buffer
   - 0,5µl 0.1M DTT
   - 0,5µl Sterile, distilled water
   - 0,5µl Superscript III Reverse Transcriptase (200units/µl)
5. Gently resuspend the mixture with the pipette and resume the PCR program: incubate at 50°C for 30–60 minutes. Increase the reaction temperature to 55°C for gene-specific primer. Reaction temperature may also be increased to 55°C for difficult templates or templates with high secondary structure.
6. Inactivate the reaction by heating at 70°C for 15 minutes.
7. After the conclusion of the program, the cDNA can be stored at -20ºC or -80ºC.

6.1.3 Quantitative PCR

Real-time quantitative PCR was performed in a 96-well plate with a final volume of 15µl per well. The protocol was the same for all target genes used: *Rp49*, *Rpl13a*, *Dscam1* and the bacterial *16S rRNA*. The list of primers can be found on the appendix 6.4. Each well contained:

- 2µl of cDNA previously diluted in 1:2
- 7,5µl of KAPA™ SYBR® Green
- 0,4µl of the forward primer at the concentration of 5µMol
- 0,4µl of the reverse primer at the concentration of 5µMol
- 4,7µl of sterile water

Firstly, was pipetted the cDNA and only after the mastermix containing all the other components. The no template controls contained 2µl of sterile water instead of cDNA. The wells were pipetted one by one and under sterile conditions on the laminar flow hood. The amplification protocol is described below, as in **(Futo et al. 2015)**:

1. Pre-incubation (1 cycle): 95ºC for 3 minutes.
2. Amplification (40 cycles): 95ºC for 10 seconds, 58ºC for 20 seconds and 72ºC for 2 seconds with fluorescence acquisition performed in each cycle at 72ºC.
3. Melting curve: 95ºC continuous.
4. Cooling down: 37ºC for 2 minutes.

6.1.4 dsRNA production

Prior to this protocol, the plasmids were already prepared and were diluted in 1:100. Three different constructs were used: Dscam-exon12; Dscam-exon15; and asnA. The first step of the dsRNA production is to amplify through a PCR as described in **(Bucher 2009)**. Add the following components to a nuclease-free water microcentrifuge tube for a final volume of 22µl:

- 2µl Plasmid template diluted at 1:100
- 8,1µl nuclease-free water
- 2,4µl MgCl at 25mM

- 4µl 5x Reaction buffer
- 2µl dNTP at 2mM
- 1µl G5 Primer at 5pmol/µl
- 1µl G4 Primer at 5pmol/µl
- 0,5µl Taq polimerase

The PCR protocol is the following:

- 1 cycle: 94ºC for 3 minutes
- 30 cycles: 94ºC for 30 seconds and 60ºC for 30 seconds
- 1 cycle: 72ºC for 45 seconds
- 1 cycle: 72ºC for 3 minutes
- Cool down to 12º

The PCR product has to be checked in a 1.5% TBE agarose electrophoresis gel. In each well are pipetted 2µl of marker and 2µl of product previously diluted. The gel has to run during 30 minutes at 100V. If the amount and size of the PCR product is correct, the purification can take place.

Purification step

For the purification of the PCR product we use the PCR purification kit (Invitek, Inc.)

In vitro transcription

After the purification step, the RNA concentration can be measured in the NanoPhotometer™. For the in vitro transcription, only 400ng of RNA are going to be used. This step is performed with the kit MEGAscript® T7 (Ambion™):

1. In a new tube add the following components:
    - 8µl of template and nuclease-free water (400ng of PCR product)
    - 2µl of 10x Reaction buffer
    - 2µl of ATP solution
    - 2µl of CTP solution
    - 2µl of GTP solution
    - 2µl of UTP solution
    - 2µl of Enzyme mix
2. Mix very well in the vortex and keep at 37ºC with 300rpm shaking for 4-5 hours.
3. Posteriorly, the mix should look a little milky. Add to the reaction 30µl of nuclease-free water and 25µl of LiCl-Lsg and mix very well. Freeze at -20ºC overnight for precipitation.
4. Thaw and centrifuge for at 13.500rpm for 40 minutes at 4ºC.
5. A milky pellet should be visible. Remove the supernatant and add 1ml of 70% ethanol.
6. Centrifuge again at 13.500rpm for 40 minutes at 4ºC.
7. Remove the supernatant and under the laminar flow hood let it dry for around 25 minutes until all the ethanol has evaporated.
8. Resuspend in 20-40µl of PBS (injection buffer).

Annealing step

The final step is the annealing. It stabilizes the dsRNA and the smear becomes less pronounced. Prepare 100ml of boiling water and when at 95ºC place the tubes on a heating block in the bath. Reduce the wanted temperature from the bath to 20ºC and let it on. Let the tubes for 15minutes in the bath. After the annealing, the dsRNA can be measured in the NanoPhotometer® and stored at -80ºC for further use. The dsRNA should also be checked in a 1.5% TBE electrophoresis agarose gel.

6.1.5 Ethanol precipitation of RNA oligonucleotides

The following protocol was adapted from Dharmacon™ ethanol precipitation protocol:

1. Split the RNA into 400µl aliquots in 2.0mL microfuge tubes.
2. Add 50µl of 3M sodium acetate (final concentration 0.3M, pH= 5.2-55)
3. Add 1.5mL ethanol per tube.
4. Vortex 10 seconds
5. Store at -20ºC overnight
6. Centrifuge at 13.000g for 20 minutes at 4ºC
7. Pour the supernatant from the tube
8. Slowly pipette 200µl of 95% Ethanol onto the pellet
9. Pour the 95% Ethanol from the tube.
10. Dry the sample under vacuum for 10-15minutes.
11. The dry pellet can be stored at -20ºC or resuspend in an appropriately buffered RNase-free solution.

6.2 List of equipment

Table 6.1 - List of machines and equipment used.

Product	Supplier
2100 Bioanalyzer	Agilent Genomics GmbH, Waldbronn, Germany
Balance	Sartoriu AG, Göttingen, Germany
Binocular Olympus SZ60	Olympus Corporation, Tokyo, Japan
Capillary pulling machine, model PC-10	Narishige Co., LTD., Tokyo, Japan
Centrifuge 5415D	Eppendorf AG, Hamburg, Germany
Centrifuge 5417R	Eppendorf AG, Hamburg, Germany
Centrifuge 5804R	Eppendorf AG, Hamburg, Germany
Concentrator 5301	Eppendorf AG, Hamburg, Germany
Femto Jet 5247 V2.02	Eppendorf AG, Hamburg, Germany
Gel electrophorese chamber	Biorad Mini-Sub® Cell GT
Incubator	Heraeus, Kendro Laboratory Products, Hanau, Germany
Laminar flow	Thermo scientific LED GmbH, Langenselbold, Germany
Light cycler® 480	Roche Diagnostics GmbH, Mannheim, Germany
NanoPhotometer™ Pearl	Implen GmbH, München, Germany
PCR cycler Mastercycler	Eppendorf AG, Hamburg, Germany
PCR cycler Mastercycler nexus flexlid	Eppendorf AG, Hamburg, Germany
Qubit® 2.0 Fluorometer	Life Technologies GmbH, Darnstadt, Germany
Shaker New Brunswick scientific	Eppendorf Vertrieb Deutschland GmbH, New Brunswick Produkte
Vortexer Vortex genie 2	Scientific Industries Incorporation, New York, USA

6.3 List of kits

Table 6.2 - List of kits used.

Name	Supplier
Power Microbiome™ RNA isolation	MO BIO Laboratories, Inc., QIAGEN GmbH, Hilden, Germany
Superscript III Reverse Transcriptase	Invitrogen by Life Technologies GmbH, Darmstadtt, Germany
MEGAscript® T7 Transcription	Ambion™ by Life Technologies GmbH, Darnstadt, Germany
Qubit RNA HS Assay	Life Technologies GmbH, Darnstadt, Germany
PCR purification kit	Invitek part of STRATEC Molecular, GmbH, Berlin, Germany

6.4 List of Primers

Table 6.3 - Primer sequences used in the study. Efficiencies (E) are given for primers that were used for RTqPCR. An arrow within primer sequences indicates where an intron lies within a RTqPCR primer.

Organism	Name	Gene accession number	Use	Efficiency	Fragment length (bp)	5‘-3’primer sequence	Primer origin
T. castaneum	*Down syndrome cell adhesion molecule 1*	TC012539	RTqPCR	2.000	83	F: AGGGCTACTG↓GGGTTTCACC R: GTAAGAGTGCCGTCTTCGA	(Peuß et al. 2016)
			RNAi D-ex12	-	145	F: CGGCGATTACAAAGATTTCAA R: AACTGCAGATAATCCTGATCCAA	(Peuß et al. 2016)
			RNAi D-ex15	-	282	F: CGGAGGCTCCAATCGCCGTT R: TCGACGGTTGCCCTTCTCCA	(Peuß et al. 2016)
	Ribosomal protein 49	TC006106	RTqPCR	1.955	132	F: TTATGGCAAACTCAAA↓CGCAAC R: GGTAGCATGTGCTTCGTTTTG	(Eggert et al. 2014)
	Ribosomal protein L13a	TC013477	RTqPCR	2.000	186	F: GGCCGCAAG↓TTCTGTCAC R: GGTGAATGGAGCCACTTGTT	(Peuß et al. 2016)
E. coli	*Asparagine synthetase A*	ECK3738	RNAi	-	304	F: ATGGRGGCGGCAATACGTGGATC R: GATTACTCCATCGCAGAAGCTGC	(Peuß et al. 2016)
Bacteria	*16S rRNA (V5-V6 region)*	-	RTqPCR	1.900	315	F: AACMGGATTAGATACCCKGG R: GCAACGAGCGCAACCC	(Hanshew et al. 2013)

6.5 Supplementary data

6.5.1 - Larvae survival four days after injections (Preliminary experiment 3.1.4)

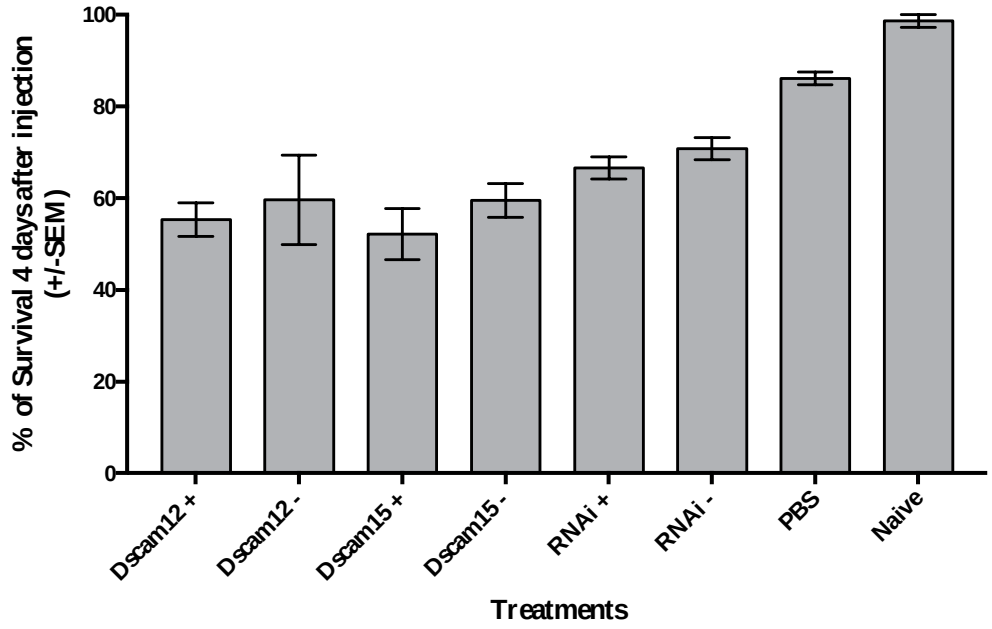

Figure 6.1 - Larvae survival four days after injections. Each treatment was composed by 72 individuals. The graphs show group mean survival plus standard error of the mean. Overall, lower dsRNA concentration treatments show a slight higher survival compared to the higher dsRNA concentration treatments.

6.5.2 - Survival for each treatment/developmental time-points (Experiment 3.2)

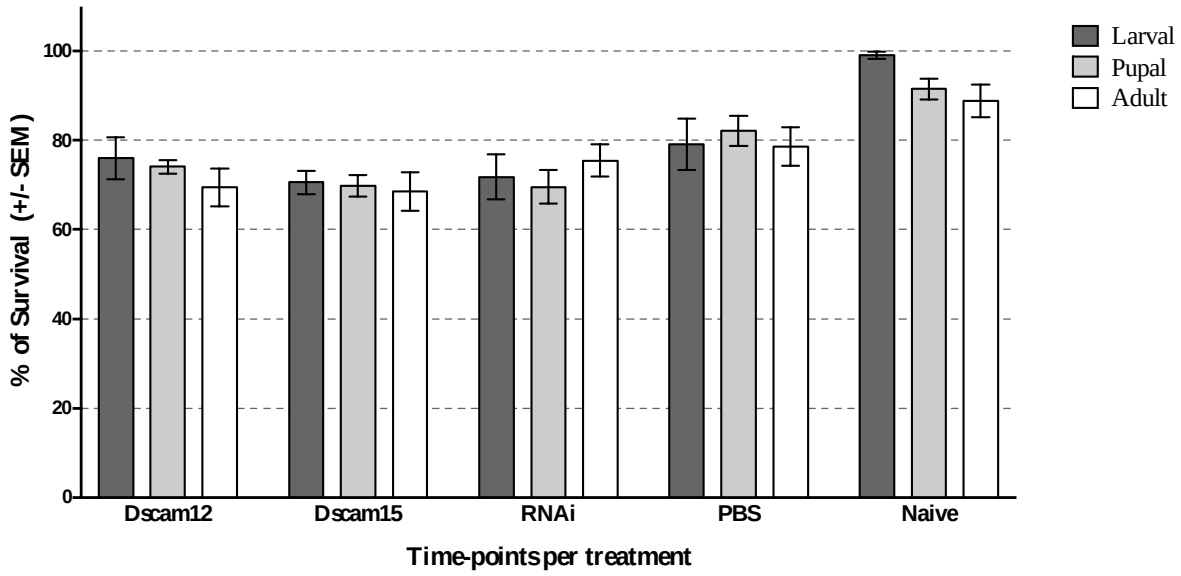

Figure 6.2 - Survival for each treatment at different beetle developmental time-points. Each combinatorial treatment was composed by 120 individuals. The graphs show group mean survival plus standard error of the mean.

6.5.3 - *Dscam1* knock-down statistics at each developmental time-point

Table 6.4 - P-value and knock-down efficiency for each treatment on each time-point. The p-value and percentage of *Dscam1* knock-down were calculated through REST statistics, while the fold change was calculated through the Ct comparative method.

Treatments	*Larval*			*Pupal*			*Adult*		
	p-value	**Fold change**	**% KD**	**p-value**	**Fold change**	**% KD**	**p-value**	**Fold change**	**% KD**
Dscam-ex12	0.043	3,48	62,9	0.007	7,61	87,0	0.004	2,31	56,1
Dscam-ex15	0.008	4,20	73,0	0.005	4,33	76,7	0.033	3,10	67,9

6.6 Abnormal RTqPCR *Rp49* amplification curve

SYBR green I is a type of dye widely used in qPCRs that forms a complex with the DNA capable of absorbing blue light and emit green light **(Zipper et al. 2004)**. All the qPCR protocols were optimized for the KAPA SYBR® FAST dye (Kapa Biosystems). Unfortunately, this specific SYBR green I became temporarily unavailable and we started to try other companies dyes, such as PerfeCTa SYBR® Green SuperMix (Quantabio). However, *Rp49* amplification curve exhibited an unusual signal (Figure 6.3). The curve presented a bump in the end of the exponential phase, as well as a slower growth. Since, we do not know if this bump would affect our data, we decided to try to solve this problem. The several tests performed to answer this problem are synthesized in Figure 6.4 and described in the sections below.

6.5.1 Can it be a problem with the primers binding during the reverse transcription or the qPCR?

At first, we hypothesized the bump in the exponential phase could be due to the formation of primer dimers. Primer dimers are a common PCR by-product, result of the hybridization of both PCR primers caused by complementary bases in each of the primers. However, in a primer dimerization scenario, the product would most likely be detected in the qPCR melting curve at a lower temperature than the specific qPCR product. The qPCR melting curves did not show any abnormality and were in agreement with what was expected. Therefore, we refuted the primer dimerization hypothesis.

Another hypothesis would be that the bump could be caused by an inappropriate binding between the cDNA fragment and the *Rp49* qPCR primers pair. This could be caused either by a problem during reverse transcription (RT), compromising the cDNA fragments, or with the qPCR primers pair that is unable to bind correctly to the cDNA fragments. In order to answer this hypothesis, we ran a new qPCR for *Rp49* with cDNA produced through RT of RNA with random hexamers and oligo(dT) primers. Three different RNA samples were analyzed. Each one was extracted from ten 15-days old larvae.

In this project, we usually only use random hexamers primers during RT because we are interested in the expression of a bacterial gene, *16S rRNA*. Bacterial mRNA usually does not possess a poly(A) tail, so the oligo(dT) are incapable of binding to them. On the other hand, random hexamers primers are 6 base-pairs random sequences that are able to randomly anneal in diverse points of a RNA molecule. Nonetheless, with this experimental set we wanted to: i) test if the *Rp49* bump was a one-time problem and with a new RT with a different batch of random hexamers primers we would be able to resolve the problem; and ii) performing a RT with oligo(dT) primers would result in more specific cDNA fragments that would perform better in the qPCR.

The 2^{-Ct} values from the qPCR are illustrated in the figure 6.5. A higher value of 2^{-Ct} corresponds to a higher gene expression. cDNA from RT with random hexamers and cDNA from RT with oligo(dT) show a similar difference across all the samples. As expected, the oligo(dT) primers performed better than the random hexamers primers for the beetle mRNA. This can be explained by the fact that during
the RT with oligo(dT) we are only amplifying mRNA with poly(A) tail and no other types of RNA. While during RT with random hexamers primers, all the total RNA is amplified. Nonetheless, the *Rp49* amplification curve still displayed the abnormal bump, suggesting the problem may not be related to the primer binding itself.

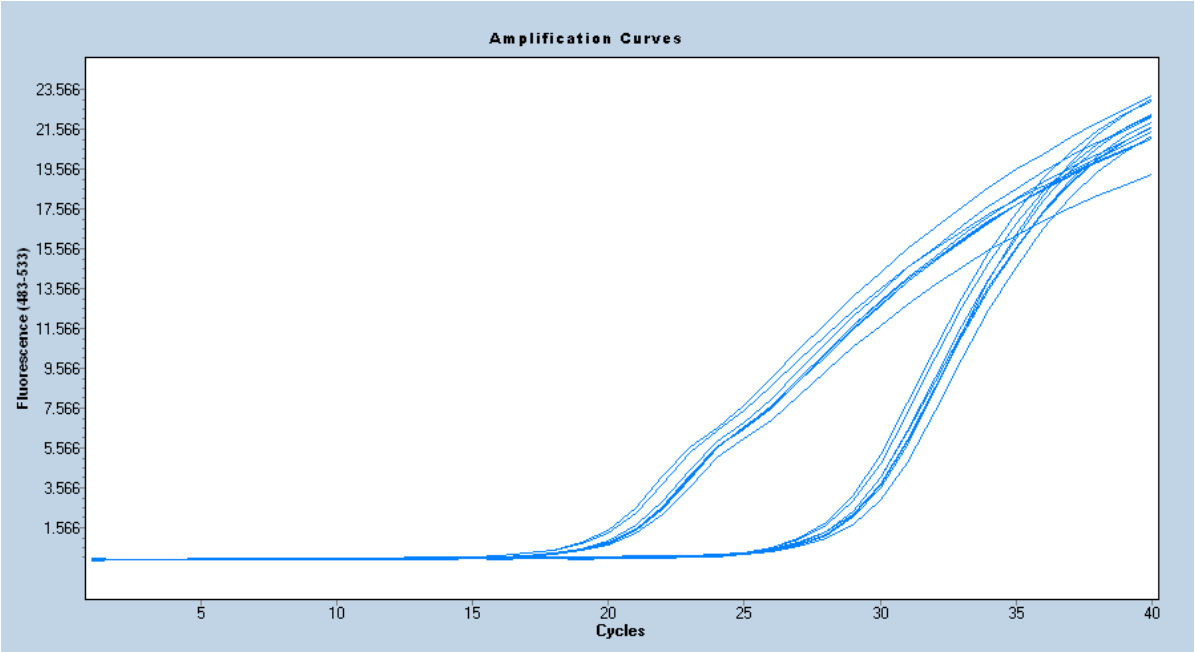

Figure 6.3 - Abnormal RTqPCR amplification curve for *Rp49*. Two clusters of amplification curves are represented. The first one group is *rp49*, while the second one is *Dscam1* for the same group of samples. Rp49 amplification curves exhibit an unusual bump that might be indicative of a problem with the new SYBR green I dye These curves were obtained using PerfeCTa SYBR® Green SuperMix (Quantabio). In the y-axis the fluorescence is represented, while in the x-axis the number of the cycles is plotted.

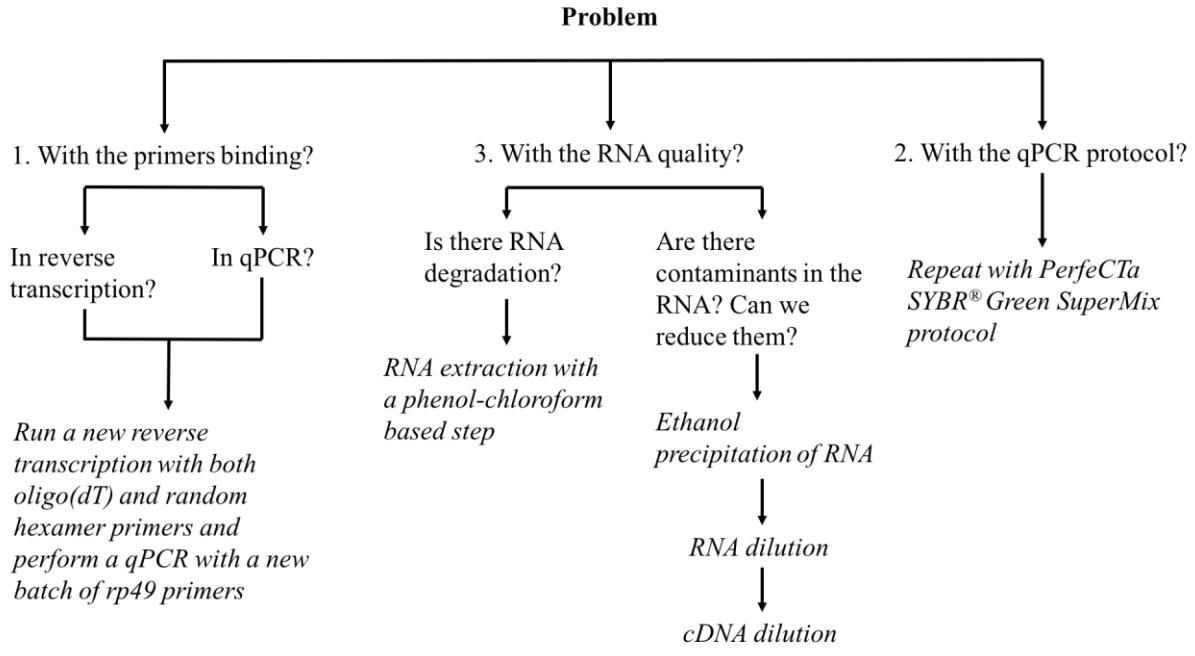

Figure 6.4 - Schematic illustration of the different steps during the troubleshooting on the problem with *Rp49* amplification curve.

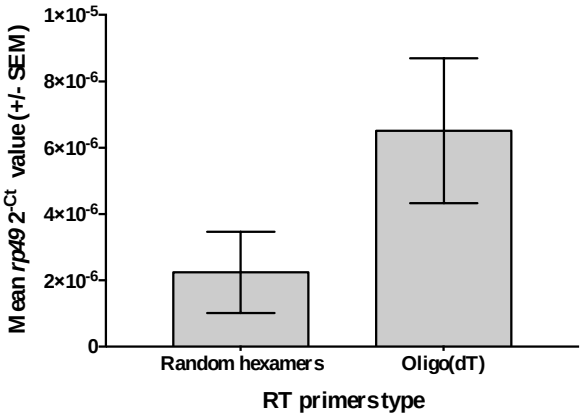

Figure 6.5 - Mean *rp49* expression of three samples after reverse transcription using random hexamers or oligo(dT) primers. The gene expression was calculated as 2^{-Ct}. The geometric mean of the 2^{-Ct} was calculated for the three samples in each RT primer treatment. A higher mean 2^{-Ct} value corresponds to an average higher expression of the gene. cDNA from a RT with random hexamers have lower 2^{-Ct} values compared to the cDNA from a RT with oligo(dT) for the same sample. As expected, the qPCR signal appears earlier through the use of oligo(dT).

6.5.2 May the new SYBR green require different protocol conditions?

The next hypothesis we formulated was that a new SYBR green I solution would probably require a different qPCR protocol and a non-optimum one could result in an abnormal amplification as this case. Therefore, we compared the qPCR protocol we use in the project, previously optimized for the amplification of the bacterial *16S rRNA* in **(Futo et al. 2015)** with the protocol from the unavailable SYBR green I solution (KAPA SYBR® FAST) and the new solution (PerfeCTa SYBR® Green SuperMix). The protocols can be found in Table 6.5. By the direct comparison between protocols we can observe that they mostly diverge on the primer dependent and extension steps. The optimized protocol is more similar to KAPA SYBR® FAST because it was optimized for that particular solution. The next step was to run a qPCR with the new SYBR green I solution protocol for three samples with a RT with random hexamers primers.

Unfortunately, the abnormal amplification curve was still present for *Rp49*. The Cp values for each of the samples did not differ from previous qPCR for the same samples. In short, the qPCR protocol did not have a significant effect on the qPCR and consequently we assumed the problem was not due to the qPCR protocol itself.

Table 6.5 - Comparison between the different qPCR protocols. The first protocol was optimized in **(Futo et al. 2015)** for the best signal amplification of the bacterial 16S rRNA with the KAPA SYBR® FAST protocol. The differences between PerfeCTa SYBR® Green SuperMix protocol and the other two mainly concerns the primer dependent and extension steps.

	Optimized for bacterial 16S rRNA(Futo et al. 2015)	**KAPA SYBR® FAST protocol**	**PerfeCTa SYBR® Green SuperMix Protocol**
Initial denaturation	95ºC, 3min	95ºC, 3min	95ºC, 3min
Amplification	95ºC, 10s	95ºC, 10s	95ºC, 10 to 15s
Primer dependent	58ºC, 20s	optional	-
Extension	72ºC, 2s	72ºC, 1s	60ºC, 30 to 60s

6.5.3 May it be a problem related with the RNA quality itself?

In this project, the RNA was extracted with the Power Microbiome™ RNA isolation kit. This kit was previously selected in **(Futo et al. 2015)** by its good performance on extracting both beetle and bacterial RNA. Nonetheless, the kit is optimal for single cells and not whole-body samples as the ones used in this study. Therefore, it may be possible the RNA isolated with this kit may not have the best quality. Several tests were performed in order to assess the RNA quality and if this may explain the abnormal *Rp49* amplification curve obtained in the qPCR. The tests are described in next sections.

6.5.3.1 RNA degradation

For a quick assessment of the RNA quality, a 1,5% TBE agarose gel was performed for five samples. As the ones analyzed before, each sample was composed by RNA from ten 15-day old larvae. The RNA quantity in each gel well was standardized to 400ng and the gel was run during 60 minutes at 60V. A negative control (N) with water instead of RNA was added to the run. The result of the run is described on figure 6.6 and a DNA ladder was used because of the unavailability of a RNA ladder. Although, we cannot confirm the RNA bands size with a DNA ladder, the rRNA bands can still be identified and other pertinent information can be obtained from this TBE gel. The upper band lightly present in the first two samples and the lower band are most likely 28S rRNA and 18S rRNA, respectively. This can be verified by their correct 2:1 size ratio. Since DNA has the double of the mass of the RNA, we could estimate 1000bp in the DNA ladder actually correspond to 2000nt of RNA, what is the average size of the 18S rRNA. Nonetheless, RNA easily forms secondary structures and we cannot be completely sure about these assumptions. The missing 28S rRNA band (upper band) and the intense smear throughout most samples is a strong sign of RNA degradation. Although smear in a gel may also be indicative of genomic DNA contamination, the fragments in the smear would be much heavier than 28S rRNA and that is not the case. Another likely scenario that may partially explain this result is a high prevalence of contaminants like salts and lipids that are known to mask RNA bands in electrophoresis gels and interfere with the binding of primers during qPCR.

For a more thorough assess of the RNA degradation, we decided to run a subset of the latter samples in the 2100 Bioanalyzer: samples 1, 2 and 3. A fourth sample was added to the subset in order to understand if the RNA degradation was a problem from this RNA extraction alone or common to all the RNA extractions performed with this methodology. This sample comes from an earlier RNA isolation followed with this exact same methodology: sample R3. Prior to the analysis, a denaturation step of 2 minutes at 70ºC was performed for all the RNA samples, as suggested in the 2100 Bioanalyzer handbook.

The electrophoregram obtained from the analysis is presented on figure 6.7. The results obtained from this analysis seem to be in concordance with the TBE gel performed previously (Figure 6.6). The big amount of smaller peaks found between the ladder (25nt) and the 18S rRNA (2000nt) is representative of some degree of RNA degradation. This degradation seems to be present throughout all the samples, suggesting that it maybe universal for all the samples extracted with this methodology. Moreover, the 28S rRNA peak is not visible in the electrophoregram. Although, 28S rRNA missing is a first sign of RNA degradation, we cannot be sure it is actually missing. A study **(Winnebeck et al. 2010)** has shown that the denaturation step prior to the analysis causes a fragmentation of the insect 28S rRNA into two domains (α and β). Therefore, the peak observed at 2000nt may represent both 18S rRNA and the two domains of 28S rRNA. Nonetheless, the RNA degradation across all the samples is undeniable and it could be the source of the qPCR amplification curve problem.

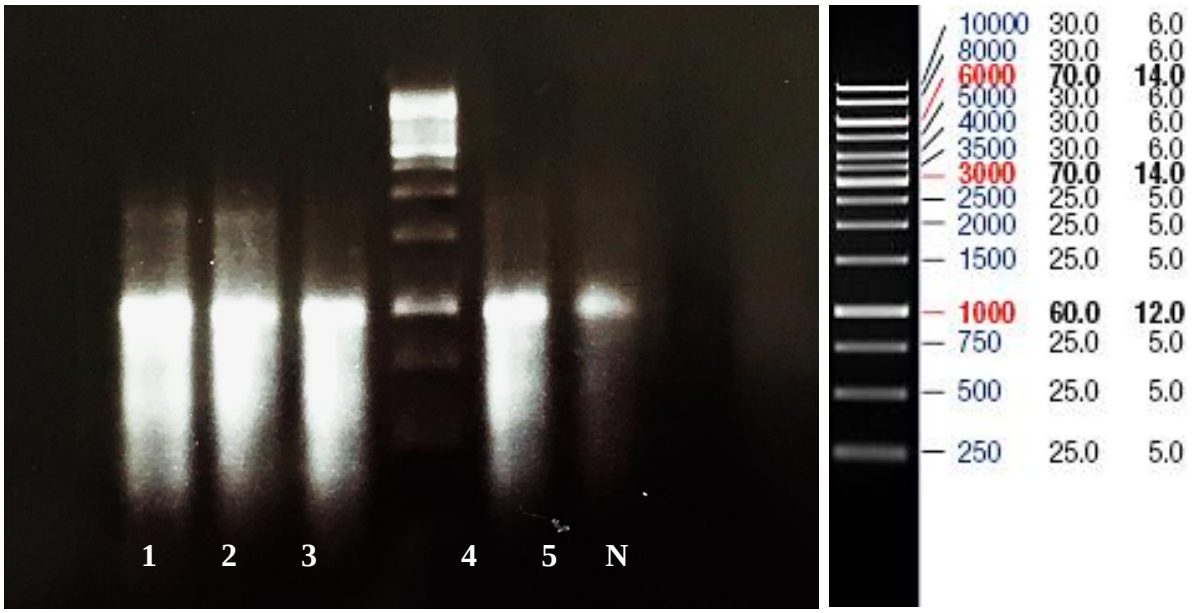

Figure 6.6 - 1.5% TBE agarose gel for 400ng of RNA samples. Five samples composed by RNA from ten 15-day old larvae were used. A negative (N) with water instead of water was added to the run. The RNA quantity in each well is standardized to 400ng and was ran during 60 minutes at 60V. The smear found in the gel is representative of RNA degradation. It was used a DNA ladder in this electrophoresis, represented at the right of the gel.

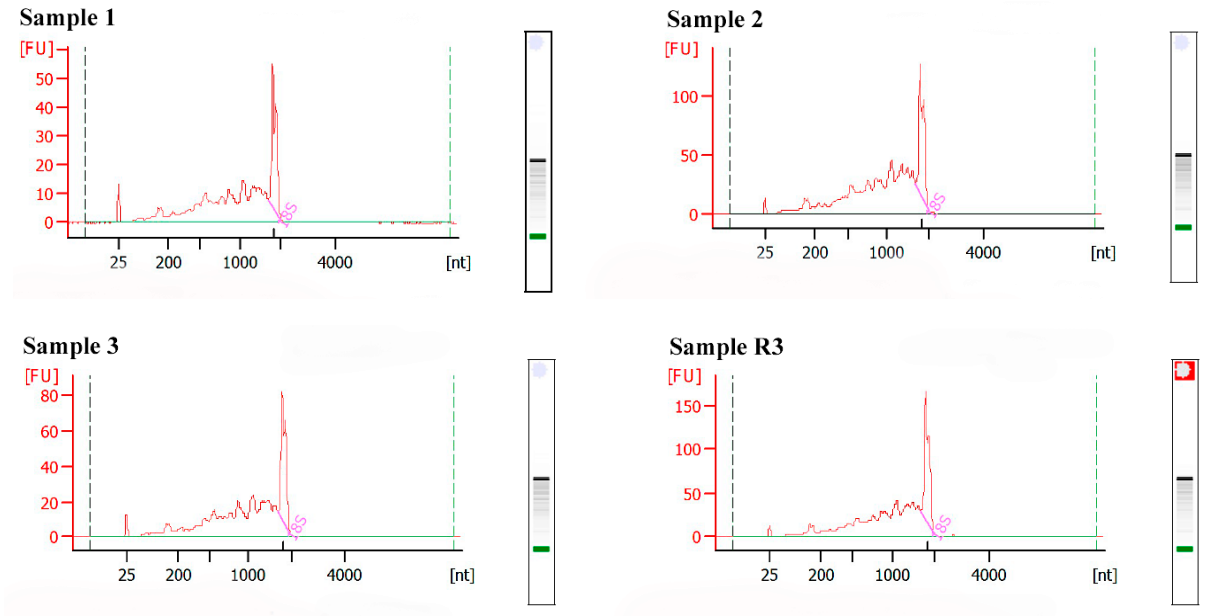

Figure 6.7 - Electrophoregram output from 2100 Bioanalyzer for the RNA samples 1, 2, 3 and a older one, R3. All the samples were extracted with the same RNA isolation protocol but RNA in R3 was obtained in a previously isolation. A denaturation step of 2 minutes at 70ºC was performed prior to the analysis as suggested in the 2100 Bioanalyzer handbook. In insects, the denaturation step is thought to cause a fragmentation of the 28S rRNA **(Winnebeck et al. 2010)**. The big peak found around 2000nt represents two 28S rRNA domains (α and β) overlapping with 18S rRNA in each sample. On the right of each graph there is a digital gel representation of the run.

The next step was to try to produce a better-quality RNA. For this, we decided to use an additional step with phenol:chloroform:isoamy alcohol during RNA extraction. We hypothesized that this additional step would reduce the potential RNA-protein complexes that may exist in the samples and result in a clearer separation between both nucleic acids and the rest of the cell components, lowering the risk of degraded RNA. For this, the RNA of three samples of ten 15-day old larvae were extracted with the phenol-chloroform based step prior to the RNA extraction, while other three were extracted without it. The samples extracted with the phenol-chloroform based step were named P1, P2 and P3, while the others without it were called NP1, NP2 and NP3.

After the extraction, the RNA concentration was measured with the NanoPhotometer™ and the Qubit®. Although, the Qubit® is thought to be more accurate in RNA concentration measurements, we also use the NanoPhotometer™ to obtain the absorbance ratios A260/280nm and A260/230nm, informative of the sample quality. The absorbance ratios were inside the appropriate intervals. The concentrations obtained are listed in Table 6.6. Curiously, a difference between the samples was already noticed upon this step. A disparity between the two methods was always found but in samples extracted with a phenol-chloroform based step, the difference between the two measurements is quite lower. While the maximum difference in "phenol" samples is 2.8ng/µl, in the "no phenol" samples is 54.0ng/µl. This may be explained by a reduction of contaminants in samples extracted with phenol, comparatively to the ones with an extraction without phenol-chloroform based step. The contaminants may cloud the measurements, resulting in higher concentration values.

Next, two samples of each treatment were run in the 2100 Bioanalyzer. This time, no denaturation step was performed prior to the analysis. The electrophoregram obtained in the analysis is represented in Figure 6.8. Since we did not perform any denaturation, the 28S rRNA peak is now observed, as expected. Both 18S rRNA and 28S rRNA show the expectable size, respectively 2000nt and 4000nt. The 28S rRNA lower peak, as well as the small peaks between both rRNAs are a sign of light degradation. Nonetheless, when compared the samples extracted with a phenol-chloroform based step (P1 and P2) with the ones without it (NP1 and NP2), it seems clear the additional step contributes to a better-quality RNA with less overall degradation. In both NP1 and NP2, we can observe a big amount of peaks of smaller sizes, as well as the absence and/or lower fluorescence peaks of rRNAs, suggesting their degradation.

Additionally, we ran a 1,5% TBE agarose gel to observe if we would get similar results to the 2100 Bioanalyzer. The RNA quantity in each well was standardized to 350ng. The gel ran at 60V for 60 minutes. A negative control (N) with water instead of RNA was added to the run. The TBE gel can be found in figure 6.9, as well as the digital gel provided in the last 2100 Bioanalyzer analysis. In both gels, less RNA degradation can be found in the "phenol" samples, comparatively to the "no phenol" ones. Also, in the "phenol" samples the 28S rRNA is also present and clearer.

Given the better results with the phenol-chloroform based step, we decided to proceed with this methodology. The next step was to perform a RT with 500ng of RNA and random hexamers primers and ran a qPCR for both group of samples. Although, there was less variability between the samples extracted with the phenol-chloroform step, the abnormality in the *Rp49* amplification curve still remained exactly the same across all the samples.

Table 6.6 - RNA concentration of samples extracted with and without the phenol:chloroform:isoamy alcohol step during RNA isolation. For each sample, the RNA concentration was measured with both NanoPhotometer™ and the Qubit®. In all the samples the absorbance ratio for A260nm / 280nm is between 2.0-2.1 and for A260nm /230nm is between 1.2-1.8. The difference between both measurements is presented below.

Samples	NanoPhotometer™ RNA concentration (ng/µl)	Qubit® RNA concentration (ng/µl)	Difference between NanoPhotometer™ and Qubit® measurements (ng/µl)
Phenol 1 (P1)	46.2	48.0	1.8
Phenol 2 (P2)	55.8	53.0	2.8
Phenol 3 (P3)	41.0	40.4	0.6
No Phenol 1 (NP1)	66.1	88.2	22.1
No Phenol 2 (NP2)	100	154	54.0
No Phenol 3 (NP3)	86.5	67.8	18.7

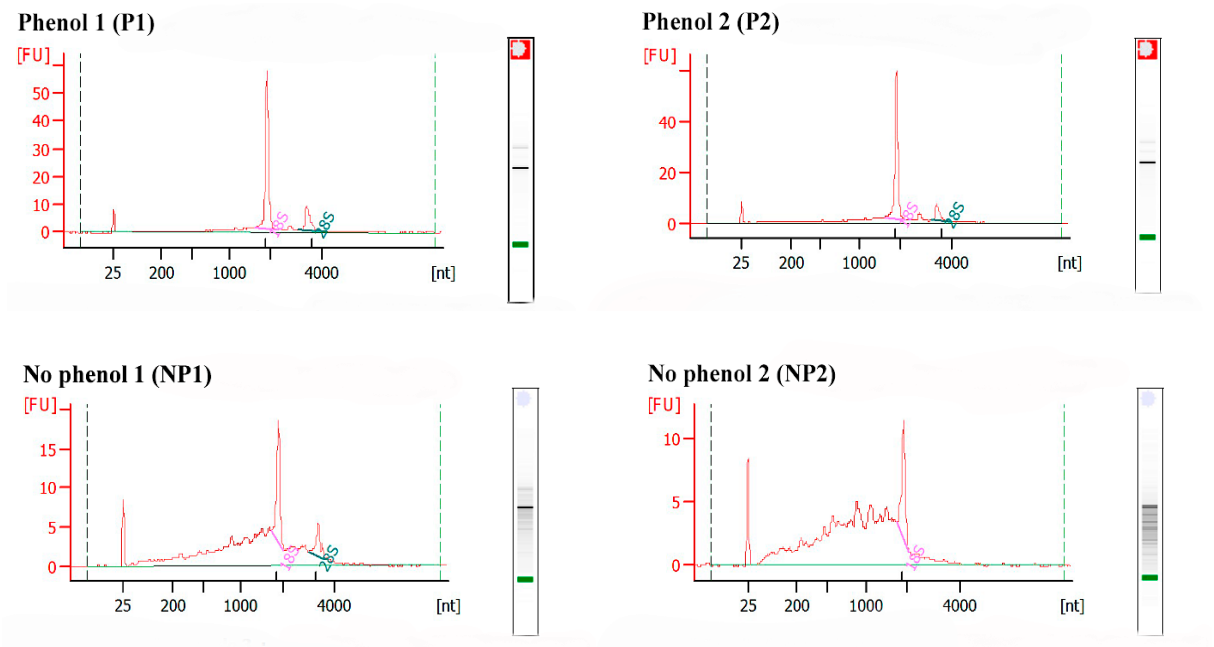

Figure 6.8 - Electrophoregram output from 2100 Bioanalyzer for the RNA samples extracted with and without the phenol:chloroform:isoamy alcohol step during RNA isolation. The samples *Phenol1* and *Phenol2* were isolated with the phenol:chloroform:isoamy alcohol step during RNA isolation with the PowerMicrobiome™ RNA isolation kit. The samples *No Phenol1* and *No Phenol2* were extracted without the phenol-chloroform based step. The samples were not subjected to a denaturation step prior to their analysis. The peak found around 2000nt represents the 18S, while the 4000nt is 28S rRNA in each sample. On the right of each graph there is a digital gel representation of the run. Samples without the phenol-chloroform based step exhibit a higher degree of RNA degradation.

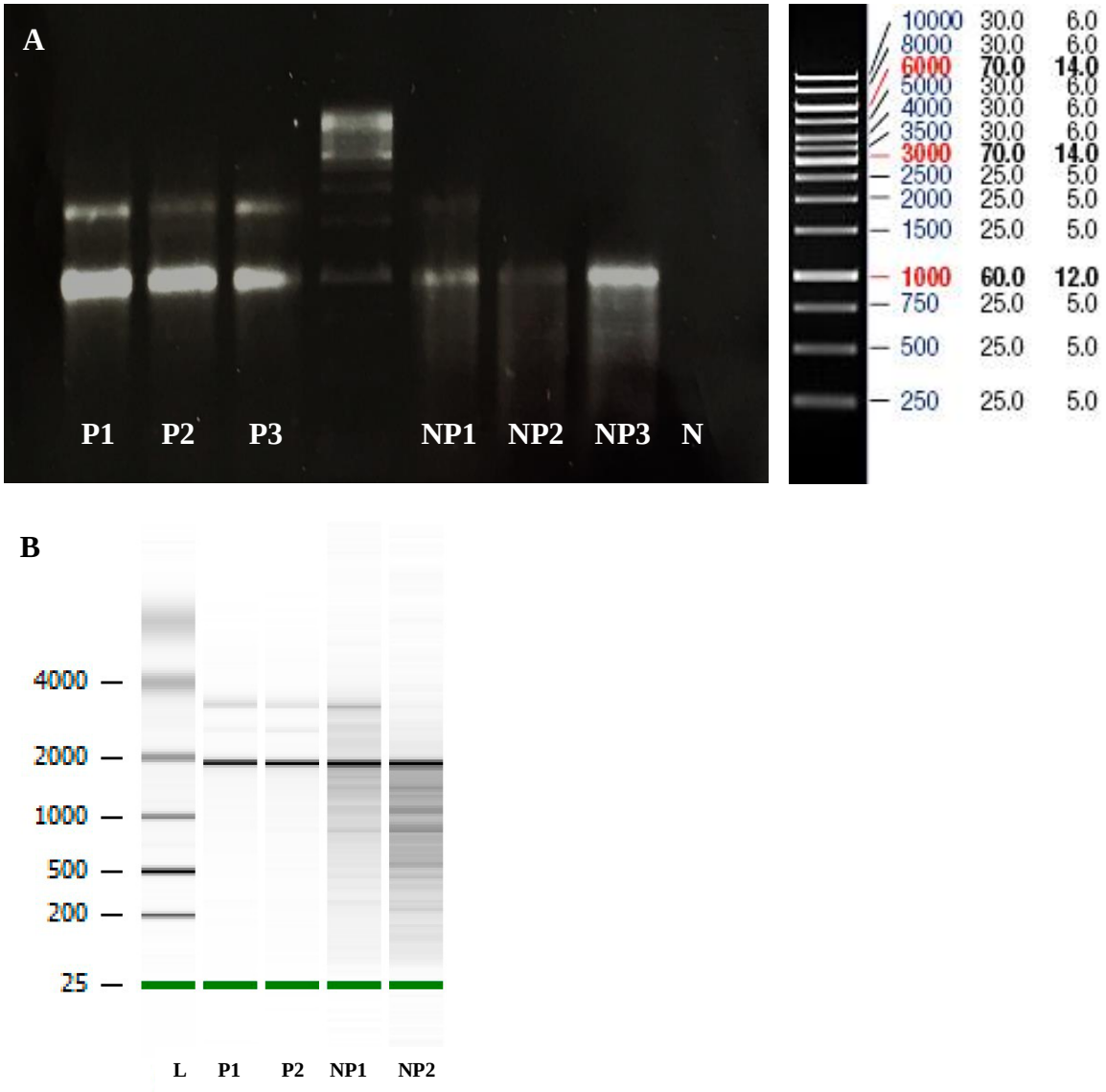

Figure 6.9 - 1.5% TBE agarose gel and 2100 Bioanalyzer output for RNA samples extracted with and without the phenol-chloroform based step during RNA isolation. Three samples extracted with the phenol-chloroform based step were run: P1, P2 and P3. P1, P2 and P3 are respectively Phenol 1, Phenol 2 and Phenol 3 mentioned before. Three other samples were extracted without the phenol-chloroform based step: NP1, NP2 and NP3. NP1, NP2 and NP3 are respectively No Phenol 1, No Phenol 2 and No Phenol 3 as described before. **(A)** A negative (neg) with water instead of water was added to the run. The RNA quantity in each well is standardized to 350ng and was ran during 60 minutes at 60V. The smear found in the gel is representative of RNA degradation. For the samples isolated with the phenol-chloroform based step is clear two bands: 18S and 28S rRNA. **(B)** Digital gel representation from the analysis ran in the 2100 Bioanalyzer. Samples without the phenol-chloroform based step show more smear, representative of RNA degradation. The result is concordant with the one obtained with the 1.5% TBE agarose gel.

6.5.3.2 RNA contamination

Though the RNA degradation got reduced, that did not have any effect in the abnormal amplification curve in the qPCR. As we mentioned before, it is possible the RNA samples had a big concentration of contaminants with lipidic nature, salts or even organic inhibitors. Since the absorbance ratio A260/230nm was significantly higher than 1.0, the presence of organic inhibitors, such as guanidine salts, that could affect the qPCR results were unlikely. Nonetheless, this and/or many other contaminants could still be present in the total RNA sample. Therefore, we thought it would be important to try an ethanol precipitation of RNA oligonucleotides. The ethanol precipitation protocol can be found in section 6.1.5. However, the precipitation step did not work. This may have happened because of the low concentration of RNA that we obtain from this RNA isolation methodology, insufficient for a precipitation step.

Next, we hypothesize that if we reduced the RNA quantity in the RT we would also potentially reduce the contaminants and their interference. Hence, we performed a RT with three different amounts of RNA: 500ng, 250ng and 50ng. In this test, we used the three samples previous extracted with a phenol-chloroform step (P1, P2 and P3) at the different quantities mentioned before.

Following the RT, a qPCR took place. The 2^{-Ct} values obtained from the qPCR are illustrated in the figure 6.10. There was no difference in the *Rp49* bump across all the different RNA dilutions. Therefore, if there is any contaminant in the RNA interfering with the amplification, reducing the RNA quantity does not solve or reduces the problem.

Hence, we decided to proceed and try different cDNA dilutions. Reducing the amount of cDNA in the qPCR may reduce the possible existent contaminants in the samples that were not reduced enough with the RNA dilutions. Another reason to perform cDNA dilutions is that a possible explanation for the abnormality found in the qPCR would be template saturation in the reaction that could lead to an incorrect amplification, observed as a bump. In the project methodology, we usually perform 1:2 cDNA dilutions. However, in this test we decided to make the following ones: 1:1; 1:10; 1:100; 1:1000; 1:10000. Given the results presented in Figure 6.10, we decided to continue with the cDNA samples from 500ng and 250ng, since they show similar 2^{-Ct} values for most of the samples.

The results from the cDNA dilutions with two different groups of cDNA (from a RT with 250ng and 500ng total RNA) are plotted in Figure 6.11. As expected, the Ct values tend do decrease linearly with the increasing concentration of cDNA. With the values obtained was possible to calculate the primers efficiency for this reaction: 96% for 500ng of total RNA and 101% for 250ng. These efficiency is in the advisable efficiency interval. Nonetheless, no changes were observed in the *Rp49* bump across the different cDNA dilutions or different RNA quantities for RT.

6.5.4 Company output

Although the contact with the company took place in the beginning of the troubleshooting, we only got a more concrete answer in the late stages after discussing the methodology and tests performed with the correct technical department.

Even though they did not know what was the problem that caused a bump in *Rp49* amplification curve, they did observe that this mostly happened in AT-rich fragments. Interestingly, the fragment used in this study is significantly rich in AT, what is in concordance what the company observed in their own studies. Also, they ensured the Cp value was not affected by the abnormal curve. The latter is in agreement with the data we got from our tests where we compared the Cp values between both dyes.

Unexpectedly, the KAPA SYBR® FAST dye became available again. Since all the protocols were optimized to this particular SYBR green I and no abnormality during amplification curve was ever found with it, we decided to return to it and proceed with the experiments.

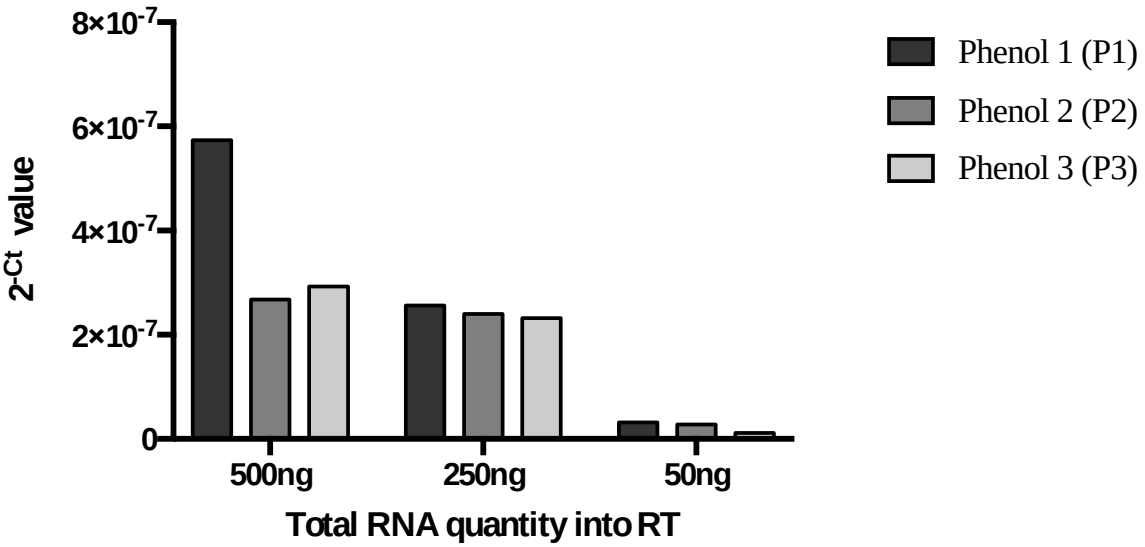

Figure 6.10 - *Rp49* expression for each of the three samples after reverse transcription with different RNA quantities. The gene expression is represented in the y-axis as 2^{-Ct}. A higher 2^{-Ct} value corresponds to a higher expression of the gene. 500ng and 250ng of total RNA into the reverse transcription show similar 2^{-Ct} values for most samples.

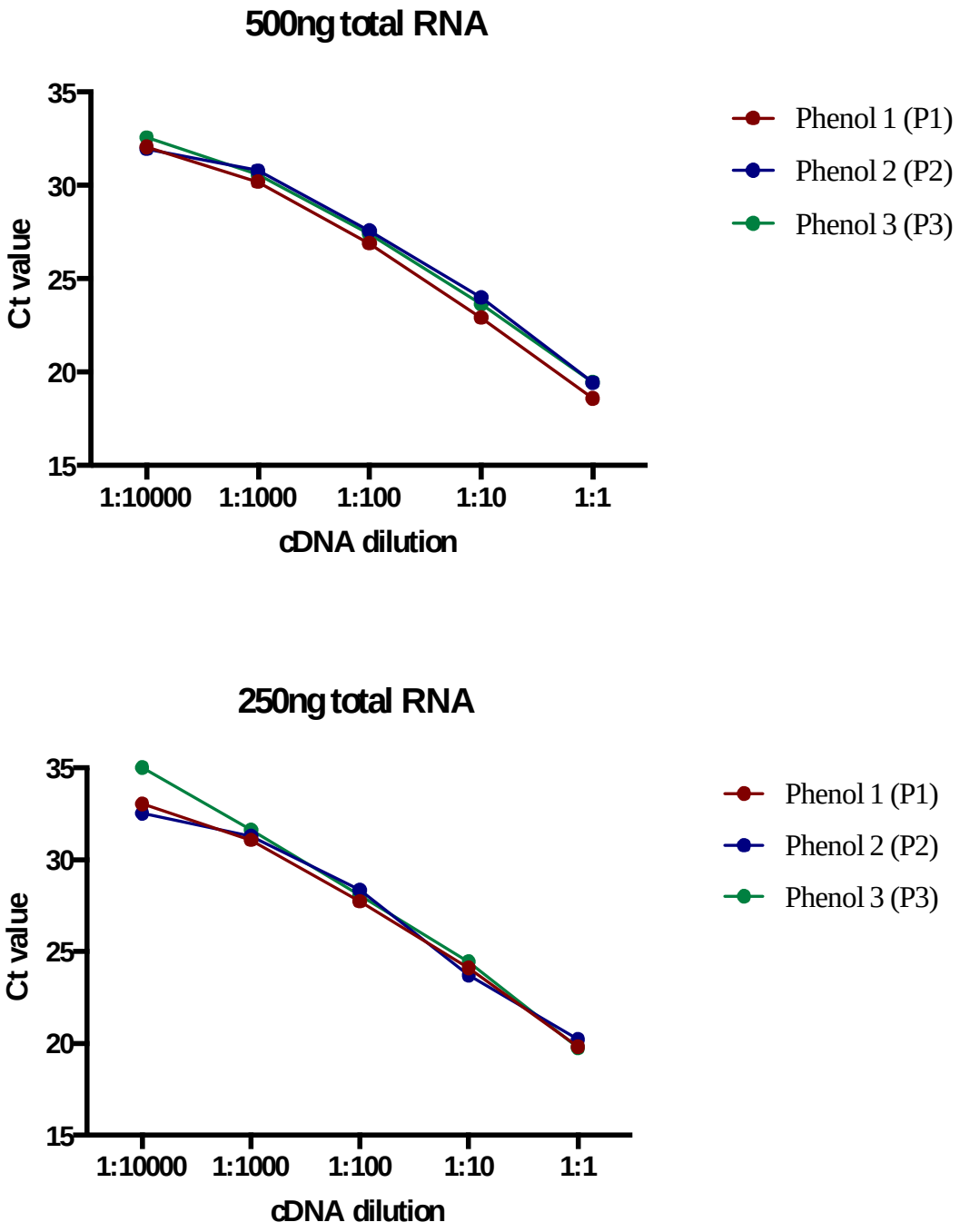

Figure 6.11 - *Rp49* expression for each of the three samples after reverse transcription of 250 and 500ng total RNA and different cDNA dilutions. The values represented are the cycle numbers obtained from the qPCR. The first graph represents the cDNA from a RT with 500ng total RNA, while the second one with 250ng total RNA. In general, the different increasingly smaller dilutions show a linear reduction in the cycle number the expression signal appears, as expected. The primers efficiency of the reaction was calculated for these values: 96% for 500ng of total RNA and 101% for 250ng.